REPORT DOCUMENTATION PAGE

Form Approved
OMB No. 0704-0188

1. AGENCY USE ONLY (Leave blank)	2. REPORT DATE 5-15-95	3. REPORT TYPE AND DATES COVERED Final Technical 1-1-92 thru 12-31-94

4. TITLE AND SUBTITLE

Stress-Stress Modelling for Heterogeneous Granular Materials Based on Micromechanics

5. FUNDING NUMBERS

AFOSR F49620-92J-0091

6. AUTHOR(S)

Ching S. Chang

7. PERFORMING ORGANIZATION NAME(S) AND ADDRESS(ES)

University of Massachusetts
Amherst, MA 01003

AFOSR-TR-95

0522

9. SPONSORING/MONITORING AGENCY NAME(S) AND ADDRESS(ES)

Air Force Office of Scientific Research
110 Duncan Ave
Suite B, 115
Bolling AFB, DC 20332-0001

N/A

10. SPONSORING/MONITORING AGENCY REPORT NUMBER

F49620-92-J-0091
N/A

11. SUPPLEMENTARY NOTES

The view, opinions and/or findings contained in this reports are those of the author(s) and should not be construed as an official AFOSR position, policy or decision, unless so designated by other documentation

12a. DISTRIBUTION/AVAILABILITY STATEMENT

Approval for public release; distribution unlimited

12b. DISTRIBUTION CODE

DTIC
SELECTED
AUG 2 2 1995
F

13. ABSTRACT (Maximum 200 words)

The objective of this research is to develop a micromechanics constitutive theory for granular material considering the effects of micro-structure. This type of micro-structural based constitutive theory is useful in many fields of studies such as in the mechanics of soil, powder, composite and ceramic. The specific efforts are focused in the following four different areas: 1) descriptions of micro-structure, 2) micro-macro relationship, 3) classes of micromechanics constitutive theory, and 4) contact law of the inter-particle binder. These four areas are the fundamental elements to the construction of a micromechanics theory for granular media. Particular attention will be given to the effect of heterogeneity in micro-structure on the micro-macro mechanical behavior. The nature of this investigation is focused on theoretical development. The developed theory is evaluated by experimental and computer simulation results.

14. SUBJECT TERMS

stress-strain model, granular mechanics, particulate mechanics, micro-structure, micromechanics

15. NUMBER OF PAGES 69 pages

16. PRICE CODE

17. SECURITY CLASSIFICATION OF REPORT	18. SECURITY CLASSIFICATION OF THIS PAGE	19. SECURITY CLASSIFICATION OF ABSTRACT	20. LIMITATION OF ABSTRACT
Unclassified N/A	Unclassified N/A	Unclassified N/A	SAR

ABSTRACT

The objective of this research is to develop a constitutive theory for granular material from a micromechanics point of view so that the effects of micro-structure are considered. This type of micro-structural based constitutive theory is useful in many fields of studies such as soil mechanics, powder mechanics, composite mechanics and ceramic mechanics. The specific efforts are focused in the following four different areas: 1) descriptions of micro-structure, 2) micro-macro relationship, 3) classes of micromechanics constitutive theory, and 4) contact law of the inter-particle binder. These four areas are the fundamental elements to the construction of a micromechanics theory for granular media.

Previous studies have shown that at large deformation, the strain exhibits non-uniformity within the material sample which contradicts to the uniform strain assumption used in the past theories. The non-uniformity of strain has been a major obstacle for constitutive modelling. Therefore, particular attention will be given to the description of heterogeneity in microstructure and the methodology of integrating the microstructure description in relating the micro-macro mechanical behavior. The micromechanics theory will lead to a model that can capture the features due to effects of microstructure and discrete nature of granular particles.

A related aspect in the development of such a micromechanics model is to find a link between discrete system and continuum system. The results of this research will provide basic understanding in different classes of continua suitable for granular materials and in the limitations of the classic continuum in the usual continuum theory. The developed theory will be evaluated by special features that exist only in granular material, such as the dispersion and decay of stress wave propagating in granular media. The nature of this investigation is focused on theoretical development. The developed theory is evaluated by experimental and computer simulation results.

DTIC QUALITY INSPECTED 3

19950821 034

i

TABLE OF CONTENTS

List of Figures

CHAPTER 1
SUMMARY OF THE PROJECT

1.1 RESEARCH OBJECTIVES

The general objective of this research is to develop a constitutive model for a packing of granules. The effort is focused in four different areas: 1) statistical descriptions of micro-structure, 2) micro-macro relationship, 3) classes of micromechanics constitutive theory, and 4) contact law of the inter-particle binder. These four areas are essential to the construction of a micromechanics theory for particulate media.

1.2 ACCOMPLISHMENTS

Accomplishments of the present project is reviewed in four different areas: 1) descriptions of micro-structure, 2) micro-macro relationship, 3) classes of micromechanics constitutive theory, and 4) contact law of the inter-particle binder.

1.2.1. Descriptions of Micro-structure

A proper description of microstructure of granular material is imperative to the modelling of its micro-scale behavior. Three approaches of microstructure description have been used. They are:
  1) particle pair (branch) model,
  2) particle group (cell or micro-element) model, and
  3) models with two-point probability function.

In the particle pair model, the configuration of each particle pair is represented by a branch. The microstructure of granular material is represented by a distribution function of the lengths and orientations of all branches. The orientational distribution is usually expressed in terms of a fabric tensor which represents the anisotropic properties of a granular media. Along this line, we studied the mechanical properties in relation to the material symmetry represented by the fabric tensor (Ref 13, 9, 12, 14, and 15 in section 1.3.3).

A more detailed description for microstructure is to divide the material into cells (e.g. Voronoi tessellations or Delaunay tessellations). Each cell represents a group of particles. Configuration of each particle group is described by a local fabric tensor. The microstructure of granular material is represented by a distribution function of the local fabric tensors. We utilize this more complex description to account for the variation of microstructure for different

1

cells (i.e., the heterogeneity of material). It was found that the effects of heterogeneity are significant on plastic deformation (Ref. 3, 4, 5, 7 in section 1.3.3).

To further describe the nature of heterogeneity, we use the two-point probability function. A new formulation is derived that determines the two-point probability function directly from the statistical measures of stereological chord length and porosity. Two-point probability function is a useful and practical descriptor for the microstructure of a general random multi-phase material. Methods are developed (24, 30) for predicting mechanical property based on the two-point probability function. Compared to the conventional effective medium theory, the two-point probability method provides a viable approach to account for the interactions among phases of material. Work continues in the area of characterizing heterogeneity by combining the concepts of (2) and (3). The objective is to search for a simple approach that captures the essential information of microstructure.

1.2.2. Micro-macro Relationship

Four methods have been used to relate micro-macro quantities.
1) kinematic hypothesis : the particle displacements are determined from macro-scale strain.
2) static hypothesis : the contact forces are determined from macro-scale stress.
3) self-consistent : the particle displacements are determined from the micro-element strain; the micro-element strain is determined from macro-scale strain based on Eshelby method.
4) statistical method : the particle displacements are determined from the micro-element strain; the micro-element strain is determined from macro-scale strain based on a statistical distribution function.

In the kinematic hypothesis, the uniform strain assumption is implied. Therefore, the derived constitutive constants are applicable only to small strain conditions where the strain is relatively uniform in a sample. At the level of large deformation, the strain becomes highly non-uniform due to particle sliding and particle rotation. When the strain field is heterogeneous, it is found that the overall behavior is no longer a straight volume average of the local behavior (Ref. 3, 4, 5, 7 in section 1.3.3).

Very few attention has been given to the heterogeneous deformation in modelling the overall behavior of the granular material. To account for the heterogeneity, the other three methods listed above for micro-macro relationship have been developed. In the formulation of static hypothesis, the derived stress-strain relationship is corresponding to a lower bound solution, in contrast to the upper bound solution from the kinematic hypothesis. Therefore, the development of a static hypothesis is useful in providing a set of bounds for estimating the exact solution. The bounds are particularly useful when the microstructure information is ·

2

limited so that an exact solution cannot be determined.

To further consider the heterogeneity, material is divided into cells (i.e. micro-elements). Configurations of cells are used to characterize the microstructure. Self-consistent method was applied to relate the micro-element strain and the macro-scale strain. Stress-strain relationship was derived based on the self consistent method, for a two dimensional granular packing considering plastic sliding (Ref. 3, 8 in section 1.3.3). The method can not be readily extended to a three-dimensional problem because it requires a Green's function for general anisotropic media which is not available for three-dimensional condition in the current literature. In this project, an effort was also devoted to the development of general Green's function (Ref. 11 in section 1.3.3). The developed three-dimensional Green's function is a useful fundamental solution that can be used not only in the self-consistent method but also in other fields of mechanics.

Statistical method was also used to relate the micro-element strain and the macro-scale strain. The canonical ensemble average technique used in statistical mechanics was adopt. The problem was addressed and the theory was derived considering particle sliding (Ref. 4, 5, 7 in section 1.3.3). Since this problem falls in the category of homogenization theory, an effective medium theory in this connection was also examined (Ref. 21, 30 in section 1.3.3).

The results show that heterogeneous strain field is a very important factor. Micro-macro relationship without consideration of heterogeneous strain field (e.g. in the kinematic hypothesis model) fails to model yielding of a packing. The three aforementioned methods are capable of modelling heterogeneous strain field and yielding of a packing. However, the static hypothesis underestimates while the other two methods overestimate failure strength. Additional work still needs to be focused in this area. Other factors associated with this problem also need to be considered such as the method of residual force redistribution due to particle sliding.

1.2.3. Classes of Micromechanics Constitutive Theory

A desirable approach is to view the system of discrete particles as a continuum. Regarding to this approach, the fundamental question is: what should be the form of the equivalent continuum? Considering the distinctive two modes of particle movements, displacement and rotation, the equivalent continuum model for the discrete system can be represented by different types of continua, for example, micro-polar continuum, high gradient continuum, non-local continuum, etc. Differed from the classic continua in solid mechanics, these continua display effects of internal characteristic length. When the particle size is relatively large compared to the sample size, the notion of classic continua is no longer adequate to represent the granular system.

3

It is clear that a micro-polar continuum captures the mode of particle rotation, thus models the consequence of asymmetric stress in granular material. It was found that the stress distribution and deformation in granular medium depend significantly on the rotation stiffness between particles (Ref. 2, 12 in section 1.3.3).

The high gradient continuum depicts the effect of high strain gradients. The model considers the strain difference of neighboring particles, thus can be regarded as a non-local model in a differential form. This type of continuum is useful in representing phenomena associated with internal characteristic length of the granular material (Ref. 14 in section 1.3.3). For example, the

high gradient medium predicts the phenomenon of decay and dispersion of short length waves (Ref. 15 in section 1.3.3).

So far, studies of the generalized continuum models show interesting singular behavior in elastic range. Plastic behavior for these continua has not yet been studied. However, it is expected that these generalized continua are useful in modelling localized deformation in plastic region due to microstructure effect. Therefore the generalized continua are potentially useful models for the plastic and after failure behavior which can not be modelled by the classic continuum.

1.2.4   Contact Law of Particles with a Binder

Most studies available in the literature are for granular materials with frictional contacts. Non-linear inter-particle contact behavior of Hertz-Mindlin type for frictional contact was used in the analysis for random packing of multi-sized granules. For particles with cemented contact such as cemented sand have been previously modeled using a adhesive-frictional contact model (Ref. 27 in section 1.3.3). However, a more realistic model for cemented contact is to view the particles connected with binders of finite thickness and finite contact area. Along this line, a theoretical model was developed for particles with elastic bonds and visco-elastic bonds.

1.3 SUMMARY OF THE PROJECT

1.3.1   Award Information

Award Number:	AFOSR F49620-92J-0091
Amount:	$ 179,964
Period:	January 1, 1992 - December 31, 1995
Title:	Stress-Stress Modelling for Heterogeneous Granular Materials Based on Micromechanics

4

1.3.2 Personnel Associated with the Project

Principal Investigator : Ching S. Chang

Research Assistants :   Gopal M. Kabir (Ph.D. completed)

Yang Chang (Ph.D. completed)

Sao J. Chao (Ph.D. completed)

Antonio J. Velez (Master's degree completed)

Joung H. Chiou (Master's degree completed)

1.3.3 Publications under the AFOSR Award

<u>Journal Publications</u>

1   Liao, C. L., and Chang, C. S., "A Micro-Structural Finite Element Model for Granular Solids," *Journal of Engineering Computations*, Vol. 9, No. 2, Pineridge Press Ltd., Swansea, U.K. 1992, pp. 267-276.

2   Chang, C. S., and Ma, L., "Elastic Material Constants for Isotropic Granular Solids with Particle Rotation," *International Journal of Solids and Structures*, Pergamon Press, Vol. 29, No. 8, 1992, pp. 1001-1018.

3   Chang, C. S., Misra, A., and Acheampong, K., "Elastoplastic Deformation of Granulates with Frictional Contacts," *Journal of Engineering Mechanics*, ASCE, Vol. 118, No. 8, 1992, pp. 1692-1708.

4   Chang, C. S., Chang, Y., and Kabir, M., "Micromechanics Modelling for the Stress-Strain Behavior of Granular Soil - I: Theory," *Journal of Geotechnical Engineering*, ASCE, Vol. 118, No. 12, 1992, 1959-1974.

5   Chang, C. S., Kabir, M., and Chang, Y., "Micromechanics Modelling for the Stress-Strain Behavior of Granular Soil - II: Evaluation," *Journal of Geotechnical Engineering*, ASCE, Vol. 118, No. 12, 1992, 1975-1994.

6   Chang, C. S., "A Discrete Element Method for Slope Stability Analysis," *Journal of Geotechnical Engineering*, ASCE, Vol. 118, No. 12, 1992, pp. 1889-1906.

7   Chang, C. S., "Micromechanics Modeling for Deformation and Failure of Granulates with Frictional Contacts," *Mechanics of Material*, Elsevier Science Publishers, Amsterdam, Vol. 16, No. 1-2, pp. 13-24, 1993.

8   Misra, A. and Chang, C. S., "Effevtive Elastic Moduli of Heterogeneous Granular Solids," *International Journal of Solids and Structures*, Pergamon Press, Vol. 30, No. 18, 1993, pp. 2547-2566.

9   Ching, C. S., and Liao, C. L., "Estimates of elastic modulus for media of randomly packed granules," *Applied Mechanics Reviews*, ASME, Vol. 47, No. 1, Part 2, 1994, pp. 197-206.

10   Chang, C. S., and Chao, S., "Discrete Element Analysis for Active and Passive Pressure Distribution on Retaining Wall," *Journal of Computers and Geotechniques*, Elsevier Science Publishers, Crown House, England, Vol. 16, 1994, pp. 291-310.

11   Chang, C. S., and Chang, Y., "Green's Function for Elastic Medium with General Anisotropy," *Journal of Appled Mechanics*, ASME, 1994 (in print).

12   Chang, C. S., and Gao, J., "Kinematic and Static Hypotheses for Constitutive Modelling of Granulates Considering Particle Rotation," *Acta Mechanica*, Springer-Verlag, 1994 (in print)

13   Chang, C.S., Chao, S. C., and Chang, Y., "Estimates of Mechanical Properties of Granulates with Anisotropic Random Packing Structure," *International Journal of Solids and Structures*, Pergamon Press, 1994 (in print).

14   Chang, C. S., and Gao, J., "Second-Gradient Constitutive Theory for Granular Material with Random Packing Structure," *International Journal of Solids and Structures*, Pergamon Press, 1994 (in print)

15   Chang, C. S. and Gao, J., "Non-linear Dispersion of Plane Wave in Granular Media," *International Journal of Non-linear Mechanics*, Pergamon Press, 1994 (in print)

Conference Proceedings

16   Lee X., and Chang, C. S., "Constitutive Modelling for Material with Perfect Disordered Heterogeneity," *ASCE Engineering Mechanics Specialty Conference*, Texas A & M University, Texas, May, 1992, pp.445-448.

17   Chang, C. S., "Probabilistic Micromechanics in Constitutive Modeling of Granular materials," *ASCE Engineering Mechanics Specialty Conference*, Texas A & M University, Texas, May, 1992, pp.437-440.

18   Chang, C.S., "Micromechanics Modelling of Deformation and Failure for Granular Material," *Advances in Micromechanics of Granular Materials*, Edited by Shen H. H. et al., Elsevier Science Publishers, Amsterdam, 1992, pp. 251-260.

19   Chang, C. S., "Microstructure Characterization in Constitutive Modelling of Granular Material," *Microstructure Characterization in Constitutive Equations in Metals and Soils*, Edited by G.Z. Voyiadjiis, American Society of Mechanical Engineers press, MD-Vol.32, 1992, pp. 55-69.

20   Chang, C. S. and Acheampong, K., "Accuracy and Stability for Static Analysis Using Dynamic Formulation in Discrete Element Methods," *Proceedings of the Second International Conference on Discrete Element Method*, March, 1993, pp. 379-389.

21   Chang Y. and Chang C. S., "Effective Moduli of Random Material," *Proceedings of the Joint ASCE/ASME/SES Conference*, June, 1993, pp. 346.

6

22   Chang, C. S., "Micromechanical Modeling for Deformation of Randomly Packed Granules," *Proceedings of the Joint ASCE/ASME/SES Conference*, June, 1993, pp. 497.

23   Chang, C. S., "Dislocation and plasticity of granular materials with frictional contacts," *Powders and Grains*, Birmingham, June 1993, pp. 105-111.

24   Chang Y. and Chang, C. S., "Effective Moduli of Random Material with Arbitrary Two-Point Joint Probability," *Homogenization and Constitutive Modeling for Heterogeneous Materials*, ASME, Applied Mechanics Division Publication Vol. 166, pp. 15-25. (Edited by Chang, C. S., and J.W. Ju.)

25   Misra, A. and Chang, C. S., "A homogenization Method for Effective Moduli of Randomly Packed Grains," *Homogenization and Constitutive Modeling for Heterogeneous Materials*, ASME, Applied Mechanics Division Publication Vol. 166, pp. 63-75. (Edited by Chang, C. S., and J.W. Ju.)

26   Chang, C. S., "Micromechanical Model for Randomly Packed Granules," *Probabilities and Materials: Tests, Models and Applications*, Cachan, France, Nov., 1993.

27   Ching, C. S. and Kabir, G. M., "Mechanism for Brittle and Ductile Behavior of Cemented Sands," *Proceedings of the Thirteenth International Conference of Soil Mechanics and Foundation Engineering*, New Delhi, India, 1994.

28   Chang, C.S., "Inter-particle Properties and Elastic Moduli for Sand," *Mechanics of Granular Material*, Published by International Society of Soil Mechanics and Foundation Engineering, 1994, pp. 7-14.

29   Chang, C. S., "Settlement and compressibility for sand under one-dimensional loading condition," *Vertical and Horizontal Deformations of Foundations and Embankments*, Edited by A. T. Yeung and G. Y. Felio, Vol. 2, ASCE, 1994, pp.1298-1311.

Dissertation and Thesis

30   Chang, Y., "Statistical Micromechanics for Effective Properties of Random Materials", Ph.D. dissertation, University of Massachusetts, 1994.

31   Velez, A. J., "Stress-Strain Model for Granular Material based on a Non-linear Contact Law", Master's project, University of Massachusetts, Dec. 1992.

32   Chao, Sao J., "Elato-plastic Stress-strain Model for Granular Material based on Static Hypothesis", Ph.D. dissertation, University of Massachusetts, 1994.

33   Kabir, G. M., "Stress-strain-strength Behavior for Granular Soils", Ph.D. dissertation, University of Massachusetts, 1992.

34   Chiou J. H., "Micro-macro Behavior of Particulate Soils with Cementation", Master's project, University of Massachusetts, Dec. 1992.

CHAPTER 2
MICROSTRUCTURE CHARACTERIZATION

Microstructure of granular material has significant effects on the macro-scale constitutive behavior. Method of microstructure characterization for granular material thus plays an important role for prediction of stress-strain relationship. Mathematical representation depends greatly on how a basic element of granular microstructure is selected. Treating the particle group as basic element, the packing structure of material can be represented by a set of particle group configurations. In this case, the basic element consists of more than two particles, thus provides more information of microstructure. Particle group represented by a Voronoi cell has been previously used in characterizing microstructure and in developing micromechanical models of granular materials (Chang et. al. 1992, Chang 1992, 1993).

In this chapter, Delaunay tessellation is discussed for microstructure characterization of granular material. The distinctive geometric feature for Delaunay cells is the tetrahedral shape, all cells composed of four faces. As oppose to the polyhedral Voronoi cells, composed of different numbers of faces, the Delaunay cells potentially are simpler to be modelled and easier to be represented statistically. Furthermore, the movement of four particles can be exactly represented by linear displacement and rotation fields. This fact makes the linear fields good representations for each tetrahedral Delaunay cell which is associated with only four particles. On the other hand, each Voronoi cell is usually associated with more than four particles. Thus artificial constraints are involved when linear fields are used for representing the movement of particles.

We seek for deriving a stress-strain relationship of a representative volume of granular material directly from the behavior of two-particle interaction. In order to account the microstructure represented by a group of particles, we view the packing structure of granular materials at three different levels, namely, 1) inter-particle contact, 2) micro-element, and 3) representative volume. Each pair of particles is regarded as the basic unit of granular material. A micro-element, which is associated with several particles, is an elementary unit at micro-scale level. At micro-element level, the discrete particle system is transformed into an equivalent continuum system and its behavior is described by the continuum concepts of stress and strain. A representative volume is defined as an assembly which contains a large number of particles to be representative of the granular material. A two dimensional schematic representation of the three levels of granular material is shown in Fig. 2.1.

In this chapter, we derive the stress-strain relationship for granular material based on micromechanics approach using Delaunay tessellation method. The derived stress-strain relationship is illustrated by comparing the predicted micro and macro behavior with computer simulation results. The predicted results are also compared for both Voronoi tessellation and Delaunay tessellation methods.

8

2.1 DISCRETE BEHAVIOR AT CONTACT LEVEL

2.1.1 Kinematics of Two Particles

Particles in this model are assumed to be stiff such that the contact deformation are small compared to the size of particles. For practical purpose, the movement of particles can be described by the kinematics of rigid particles. There are two modes of movement for a particle: translation, Δu_i^n, and rotation, $\Delta \omega_i^n$. The superscript 'n' refers to the n-th particle. Based on the kinematics of two rigid particles of convex shape as shown in Fig. 2.2, the relative displacement $\Delta \delta_i^{nm}$ and the relative rotation $\Delta \theta_i^{nm}$ of particle 'm' to particle 'n' at the contact point 'c' are given by

$$\Delta \delta_i^{nm} = \Delta u_i^m - \Delta u_i^n + e_{ijk}(r_k^{mc}\Delta \omega_j^m - r_k^{nc}\Delta \omega_j^n) \tag{2.1}$$

$$\Delta \theta_i^{nm} = \Delta \omega_i^m - \Delta \omega_i^n \tag{2.2}$$

where r_k^{nc} is the position vector measured from the center of the n-th particle to the contact point 'c' and the quantity e_{ijk} is the permutation symbols used in tensor representation for cross product of vectors. Combining tensor and matrix notation, Eqs. 2.1 and 2.2 can be written in a compact form as follows:

$$\{\Delta D_i^{nm}\} = [R_{ij}^{mc}]\{\Delta U_j^m\} - [R_{ij}^{nc}]\{\Delta U_j^n\} \tag{2.3}$$

where $\{D_i^{nm}\}$ is the generalized inter-particle displacement vector and $\{U_j^n\}$ is the generalized particle-displacement vector. $\{D_i^{nm}\}$, $\{U_j^n\}$, and $[R_{ij}^{nc}]$ are defined as follows:

$$\{D_i^{nm}\} = \begin{Bmatrix} \delta_i^{nm} \\ \theta_i^{nm} \end{Bmatrix}; \quad \{U_j^n\} = \begin{Bmatrix} u_j^n \\ \omega_j^n \end{Bmatrix}; \quad [R_{ij}^{nc}] = \begin{bmatrix} \delta_{ij} & e_{ijk}r_k^{nc} \\ 0 & \delta_{ij} \end{bmatrix}. \tag{2.4}$$

where δ_{ij} is the Kronecker delta.

2.1.2 Inter-particle Law

Due to movement of particles, forces and moments transmit through at the inter-particle contacts. The inter-particle displacement, $\Delta \delta_i^{nm}$, and the contact force, Δf_i^{nm}, at the inter-particle contact can be expressed in a general relationship of incremental form as

$$\Delta f_i^{nm} = k_{ij}^{nm} \Delta \delta_j^{nm} \tag{2.5}$$

The contact stiffness tensor k_{ij}^{nm} is given by

$$k_{ij}^{nm} = k_n^{nm} n_i^{nm} n_j^{nm} + k_s^{nm} (s_i^{nm} s_j^{nm} + t_i^{nm} t_j^{nm}) \tag{2.6}$$

where n, s and t are the basic unit vectors of the local coordinate system construct at each contact. The vector n is the outward normal to the contact plane. The other two orthogonal vectors s and t are on the contact plane. The scaler quantities k_n^{nm} is the inter-particle

normal stiffness and k_s^{nm} is the inter-particle shear stiffness.

The inter-particle rolling and torsional stiffness transmit the inter-particle moment (couple). The inter-particle torsional stiffness is denoted by g_n^{nm} and the inter-particle rolling

stiffness is denoted by g_s^{nm}. The inter-particle relative rotation, $\Delta\theta_i^{nm}$, and the inter-particle

contact moment, Δm_i^{nm}, can be expressed in a general relationship of incremental form as

$$\Delta m_i^{nm} = g_{ij}^{nm} \Delta\theta_j^{nm} \tag{2.7}$$

The inter-particle rotation stiffness tensor g_{ij}^{nm} is given by

$$g_{ij}^{nm} = g_n^{nm} n_i^{nm} n_j^{nm} + g_s^{nm} (s_i^{nm} s_j^{nm} + t_i^{nm} t_j^{nm}) \tag{2.8}$$

Eqs. 2.5 and 2.7 can be combined into a compact form as follows:

$$\{\Delta F_i^{nm}\} = [K_{ij}^{nm}] \{\Delta D_j^{nm}\} \tag{2.9}$$

where $\{D_j^{nm}\}$ is the generalized inter-particle displacement vector, $\{F_i^{nm}\}$ is the generalized

inter-particle force vector, and $[K_{ij}^{nm}]$ is the generalized inter-particle stiffness tensor, defining

in the follows:

$$\{D_j^{nm}\} = \begin{Bmatrix} \delta_j^{nm} \\ \theta_j^{nm} \end{Bmatrix}; \quad \{F_i^{nm}\} = \begin{Bmatrix} f_i^{nm} \\ m_i^{nm} \end{Bmatrix}; \quad [K_{ij}^{nm}] = \begin{bmatrix} k_{ij}^{nm} & 0 \\ 0 & g_{ij}^{nm} \end{bmatrix}. \tag{2.10}$$

2.2 METHODS OF MICROSTRUCTURE CHARACTERIZATION

To study a granular material with randomly packed particles, a suitable model for characterizing microstructure is essential. Two simple and widely used methods in the theory of stochastic geometry are examined, namely, the Voronoi tessellation method and the Delaunay tessellation method.

10

Both methods was originally used to characterize the microstructure of a set of randomly distributed points in space, such as the two dimensional example schematically shown in Fig. 2.3a. The configuration of a set of discrete points has certain statistical similarity to that of a set of discrete particles, such as the two dimensional example schematically shown in Fig. 2.3b. Therefore, the methods for a set of points are expected to have ability for capturing, not in detail but, main features of the microstructure for a set of randomly distributed particles in space.

Both methods transform the set of points into a cell structure. Microstructure of the system is characterized through the arrangements and shapes of cells. The Voronoi tessellation method divides the space into polyhedral cells. Each Voronoi cell contains a particle point. Each face of the polyhedron separates two neighboring particles. Shape of the polyhedron represents the arrangement of a particle point and its neighbors. The Voronoi tessellation for the set of points in Fig. 2.3a is given in Fig. 2.4a. If each polyhedron cell is occupied by a particle, it is corresponding to Fig. 2.3b.

The Delaunay tessellation is a unique representation dual to the Voronoi tessellation. The Delaunay method divides the space into tetrahedral cells. Based on the vertexes of the Voronoi polyhedra, the Delaunay cell can be formed by connecting the four particle points nearest to the vertex. Each tetrahedral cell has 4 faces and 6 edges. The cell encloses a void. Each edge connects a pair of particles. The Delaunay tessellation for the set of particle points in Fig. 2.3a is given in Fig. 2.4b.

The method of Voronoi tessellation has been utilized by Chang et. al. (1992) and Chang (1992, 1993) to characterize microstructure of granular material. The Delaunay tessellation is expected to have advantages over the Voronoi tessellation in that all Delaunay cells are tetrahedra, of which the statistical information are easier to be obtained. In this chapter, we propose the Delaunay tessellation for characterizing microstructure.

2.3 DELAUNAY TESSELLATION FOR MICRO-ELEMENT

2.3.1 Strain Field in a Delaunay Micro-element

A Delaunay cell is associated with four particles. The tetrahedral micro-element is constructed by the centroids of the four particles. Define displacement and rotation fields in the micro-element as linear functions:

$$\Delta u_i(X) = \Delta u_i^e + \Delta u_{ij}^e X_j \qquad (2.11)$$

$$\Delta \omega_i(X) = \Delta \omega_i^e + \Delta \omega_{ij}^e X_j \qquad (2.12)$$

11

where X_j is the position vector measured from the centroid of the micro-element, u_i^e and ω_i^e are respectively the displacement and the rotation at the centroid of the micro-element, $u_{i,j}^e$ is the displacement gradient, $\omega_{i,j}^e$ is the rotation gradient, and the superscripts 'e' refers to the e-th micro-element.

Using continuum variables of the displacement and rotation fields, the inter-particle displacement and the inter-particle rotation in Eqs. 2.1 and 2.2 can be expressed as:

$$\Delta \delta_i^{nm} = \Delta \epsilon_{ji}^e l_j^{nm} + e_{ijk} \Delta \gamma_{ji}^e (X_l^m r_k^{mc} - X_l^n r_k^{nc}) \tag{2.13}$$

$$\Delta \theta_i^{nm} = \Delta \gamma_{ji}^e l_j^{nm} \tag{2.14}$$

where l_j^{nm} is the branch vector measured from the center of the n-th particle to the center of the m-th particle and r_k^{nc} is the position vector connecting the center of n-th particle to the contact point 'c'. The branch vector and position vectors are related by $l_j^{nm} = X_j^m - X_j^n$ or $l_j^{nm} = r_j^{nc} - r_j^{mc}$. The asymmetric deformation strain ϵ_{ji}^e and the polar strain γ_{ji}^e are defined, similar to that given by Chang and Liao (1990) and Chang and Ma (1990), as follows:

$$\Delta \epsilon_{ji}^e = \Delta u_{i,j}^e + e_{ijk} \Delta \omega_k^e \tag{2.15}$$

$$\Delta \gamma_{ji}^e = \Delta \omega_{i,j}^e \tag{2.16}$$

The symmetrical part of the strain $\Delta \epsilon_{ij}^e$ is equal to the symmetrical part of displacement gradient, representing the usual strain of the micro-element, i.e.,

$$\Delta \epsilon_{(ij)}^e = \frac{1}{2}(\Delta \epsilon_{ij}^e + \Delta \epsilon_{ji}^e) = \frac{1}{2}(\Delta u_{j,i}^e + \Delta u_{i,j}^e) \tag{2.17}$$

The skew symmetric part of the strain $\Delta \epsilon_{ij}^e$ represents the net spin of particles (i.e., the difference between rigid body rotation and the particle rotation at the centroid of the micro-element). Thus

$$\Delta \epsilon_{[ij]}^e = \frac{1}{2}(\Delta \epsilon_{ij}^e - \Delta \epsilon_{ji}^e) = \frac{1}{2}(\Delta u_{j,i}^e - \Delta u_{i,j}^e) - e_{ijk} \Delta \omega_k^e \tag{2.18}$$

It is noted that, we aim to describe the movements of discrete particles with continuum variables $\{\epsilon_{ij}^e, \gamma_{ij}^e\}$ instead of discrete variables $\{u_i^n, \omega_i^n\}$. Substituting the linear fields of

12

Eqs. 2.15 and 2.16 into Eqs. 2.11 and 2.12, particle movements and micro-element strains are related by

$$\Delta u_i(X^n) = \Delta u_i^e + \Delta \epsilon_{ji}^e X_j^n - e_{ijk}\Delta \omega_k^e X_j^n \tag{2.19}$$

$$\Delta \omega_i(X^n) = \Delta \omega_i^e + \Delta \gamma_{ji}^e X_j^n \tag{2.20}$$

where u_i^n, ω_i^n are respectively the displacement and rotation of particle n. X_j^n is the position vector from centroid of the micro-element to the centroid of particle n. Since the superscript n denotes the particles from 1 to 4 for a Delaunay cell, the set of 24 discrete variables $\{u_i^n, \omega_i^n\}$ can be fully replaced by the set of 24 continuum variables $\{\epsilon_{ij}^e, \gamma_{ij}^e, u_i^e, \omega_i^e\}$.

Neglecting the rigid body translation and the rigid body rotation, we let

$$\Delta u_i^e = 0 \tag{2.21}$$

$$\Delta u_{i,j}^e - \Delta u_{j,i}^e = 0 \tag{2.22}$$

Substituting Eq. 2.22 into Eq. 2.18, it becomes:

$$\Delta \omega_i^e = -\frac{1}{2} e_{ijk}\Delta \epsilon_{jk}^e \tag{2.23}$$

Using Eqs. 2.21 and 2.23, Eqs. 2.19 and 2.20 can now be written as follows:

$$\Delta u_i(X^n) = \frac{1}{2}(\Delta \epsilon_{ij}^e + \Delta \epsilon_{ji}^e)X_j^n \tag{2.24}$$

$$\Delta \omega_i(X^n) = -\frac{1}{2} e_{ijk}\Delta \epsilon_{jk}^e + \Delta \gamma_{ji}^e X_j^n \tag{2.25}$$

In Eqs. 2.24 and 2.25, the total number of continuum variables is 18 as represented by the set $\{\epsilon_{ij}^e, \gamma_{ij}^e\}$. With those 6 known conditions of rigid body movement (Eqs. 2.21 and 2.23), the 24 discrete variables of $\{u_i(X^n), \omega_i(X^n)\}$ can be uniquely defined from the set of 18 continuum variables $\{\epsilon_{ij}^e, \gamma_{ij}^e\}$.

It is noted that the linear field assumption used in Voronoi representation (Chang, 1992) does not lead to a unique mapping between discrete variables and continuum variables. As oppose to the Delaunay cell, a Voronoi cell usually consists of more than 4 particles, such that the number of discrete variables $\{u_i(X^n), \omega_i(X^n)\}$ are more than 24. Therefore, the linear field assumption in Voronoi representation involves artificial kinematic constraints. In this regards, linear field assumption is a better representation for Delaunay tessellation method.

13

2.3.2 Micro-element Strain versus Inter-particle Displacement

We express the relative movement of a particle pair (Eqs. 2.13 and 2.14) in terms of the generalized strain tensor $\{E_{jk}^e\}$ as follows:

$$\{\Delta D_i^{nm}\} = [L_{ijk}^{nm}]\{\Delta E_{jk}^e\} \tag{2.26}$$

where $\{D_i^{nm}\}$, as given in Eq. 2.10, is the generalized inter-particle displacement vector between particles 'm' and 'n' and $[L_{ijk}^{nm}]$ is the fabric tensor operator. $[L_{ijk}^{nm}]$ and $\{E_{jk}^e\}$ are given by

$$[L_{ijk}^{nm}] = \begin{bmatrix} \delta_{ik}l_j^{nm} & e_{ikl}(X_j^m r_l^{mc} - X_j^n r_l^{nc}) \\ 0 & \delta_{ik}l_j^{nm} \end{bmatrix}; \quad \{E_{jk}^e\} = \begin{Bmatrix} \epsilon_{jk}^e \\ \gamma_{jk}^e \end{Bmatrix} \tag{2.27}$$

Each Delaunay cell of tetrahedral shape consists of 4 vertices and 6 branch vectors (edges). Since there are 6 variables of $\{D_i^{nm}\}$ associated with each branch vector, thus the total number of variables $\{D_i^{nm}\}$ is 36 for a cell, which can be determined from 18 continuum variables of the set $\{\epsilon_{ij}^e, \gamma_{ij}^e\}$. It is noted that the 36 variables are not independent due to geometric constraint of compatibility. On the face made of 3 vertices (say, m, n, and q), the 6 variables of $\{D_i^{nm}\}$ associated with the branch vector l_i^{nm} can be expressed by the variables $\{D_i^{nq}\}$ and $\{D_i^{qm}\}$ associated with the other two branch vectors l_i^{nq} and l_i^{qm}, given by

$$D_i^{nm} = D_i^{nq} + D_i^{qm} \tag{2.28}$$

For each Delaunay cell, 18 compatibility equations can be written. The other 12 equations are:

$$\begin{aligned} D_i^{ml} &= D_i^{mq} + D_i^{ql} \\ D_i^{ln} &= D_i^{lq} + D_i^{qn} \end{aligned} \tag{2.29}$$

The inter-particle displacements obtained from the generalized strain tensor $\{E_{jk}^e\}$ using Eq. 2.26 automatically satisfy the 18 compatibility equations.

2.3.3 Inter-particle force versus micro-element stress

The stress of a micro-element can be defined using the principle of energy

14

equivalence. Due to an increment of strain, the potential energy from the stress and strain is equal to the work done at the inter-particle contacts. Note that each particle pair is the edge shared by several micro-elements. Let α^c be the number of micro-elements that share the same edge. It is noted that, for simplicity, we use the superscript 'c' to instead of the superscripts 'nm'. Assuming the work done at this contact is equally shared by all micro-elements associated with this contact. The energy equivalence is

$$\sigma_{ij}^e \Delta \epsilon_{ij}^e + \mu_{ij}^e \Delta \gamma_{ij}^e = \frac{1}{V^e} \sum_c \frac{1}{\alpha^c} (f_j^c \Delta \delta_j^c + m_j^c \Delta \theta_j^c) \tag{2.30}$$

It can be written in a compact form as follows:

$$\{S_{ij}^e\}^T \{\Delta E_{ij}^e\} = \frac{1}{V^e} \sum_c \frac{1}{\alpha^c} \{F_k^c\}^T \{\Delta D_k^c\} \tag{2.31}$$

where $\{S_{ij}^e\}$ is the generalized stress tensor given by

$$\{S_{ij}^e\} = \begin{Bmatrix} \sigma_{ij}^e \\ \mu_{ij}^e \end{Bmatrix} \tag{2.32}$$

in which $\{\sigma_{ij}^e\}$ is the Cauchy stress tensor and $\{\mu_{ij}^e\}$ is the polar stress tensor for a micro-element. It is noted that α^c is 2 for two dimensional case. In a three dimensional case, α^c is an additional measure of microstructure describing the neighbors of a micro-element.

By substituting Eq. 2.26 into Eq. 2.31,

$$\{\Delta E_{ij}^e\} \left(\{S_{ij}^e\}^T - \frac{1}{V^e} \sum_c \frac{1}{\alpha^c} \{F_k^c\}^T [L_{kij}^c] \right) = 0 \tag{2.33}$$

Since the incremental strain is arbitrary chosen, in order to satisfy the energy conservation, we have

$$\{S_{ij}^e\}^T = \frac{1}{V^e} \sum_c \frac{1}{\alpha^c} \{F_k^c\}^T [L_{kij}^c] \tag{2.34}$$

or

$$\{S_{ij}^e\} = \frac{1}{V^e} \sum_c \frac{1}{\alpha^c} [L_{kij}^c]^T \{F_k^c\} \tag{2.35}$$

More specifically,

$$\sigma_{ij}^e = \frac{1}{V^e} \sum_c \frac{1}{\alpha^c} f_j^c l_i^c \tag{2.36}$$

$$\mu_{ij}^e = \frac{1}{V^e} \sum_c \frac{1}{\alpha^c} \left(m_j^c l_i^c + e_{jlk} f_k^c (X_l^m r_l^{mc} - X_i^n r_l^{nc}) \right) \tag{2.37}$$

where $l_i^c = l_i^{nm} = X_i^m - X_i^n$. Also, $f_j^c = f_j^{nm}$ and $m_j^c = m_j^{nm}$ are the inter-particle force and moment acting on the n-th particle respectively.

2.3.4 Constitutive Law for Micro-element

The stress-strain relationship for a micro-element is given by

$$\{\Delta S_{ij}^e\} = [C_{ijkl}^e] \{\Delta E_{kl}^e\} \tag{2.38}$$

The stiffness tensor $[C_{ijkl}^e]$ can be derived from the following three essential relationships:

1) inter-particle force to micro-element stress relationship (Eq. 2.35)
2) inter-particle law (Eq. 2.9)
3) micro-element strain to inter-particle displacement relationship (Eq. 2.26)

These relationships are schematically shown in Fig. 2.5. Using these three equations, the stiffness tensor $[C_{ijkl}^e]$ is derived, given by

$$[C_{ijkl}^e] = \frac{1}{V^e} \sum_c \frac{1}{\alpha^c} [L_{mij}^c]^T [K_{mn}] [L_{nkl}^c] \tag{2.39}$$

Eq. 2.38 can be expressed as follows:

$$\begin{Bmatrix} \Delta \sigma_{ij}^e \\ \Delta \mu_{ij}^e \end{Bmatrix} = \begin{bmatrix} A_{ijkl}^e & B_{ijkl}^e \\ D_{ijkl}^e & E_{ijkl}^e \end{bmatrix} \begin{Bmatrix} \Delta \epsilon_{kl}^e \\ \Delta \gamma_{kl}^e \end{Bmatrix} \tag{2.40}$$

where

$$
\begin{aligned}
A_{ijkl}^e &= \frac{1}{V^e} \sum_c \frac{1}{\alpha^c} l_i^c k_{jl} l_k^c \\
B_{ijkl}^e &= \frac{1}{V^e} \sum_c \frac{1}{\alpha^c} e_{lmn} l_i^c k_{jn} (X_k^m r_m^{mc} - X_k^n r_m^{nc}) \\
D_{ijkl}^e &= \frac{1}{V^e} \sum_c \frac{1}{\alpha^c} e_{jmn} l_k^c k_{nl} (X_i^m r_m^{mc} - X_i^n r_m^{nc}) \\
E_{ijkl}^e &= \frac{1}{V^e} \sum_c \frac{1}{\alpha^c} \left(l_i^c g_{jl} l_k^c + e_{jpn} e_{lqm} k_{nm} (X_i^m r_p^{mc} - X_i^n r_p^{nc})(X_k^m r_q^{mc} - X_k^n r_q^{nc}) \right)
\end{aligned}
\tag{2.41}
$$

A brief summary of the discrete variables, the continuum variables, and their relationships for a Delaunay micro-element is given in Table 2.1.

16

2.4 OVERALL BEHAVIOR FOR REPRESENTATIVE VOLUME

In what follows, we derive the constitutive law for a representative volume of the granular material. The macro-level stress-strain behavior is obtained from the averaged behavior of micro-elements. The overall stress and strain, denoted by ΔS_{ij} and ΔE_{ij}, are regard as volume averages of the local stresses and local strains at the micro-element level, such that:

$$\Delta S_{ij} = \frac{1}{V} \sum_e V^e \Delta S_{ij}^e \tag{2.42}$$

$$\Delta E_{ij} = \frac{1}{V} \sum_e V^e \Delta E_{ij}^e \tag{2.43}$$

where V^e is the volume associated with the e-th micro-element. Summation over the volume V^e of all micro-elements is equal to the representative volume V.

To derive the correct overall constitutive relationship, it is essential to account for the fluctuations of local strain ΔE_{ij}^e and local stress ΔS_{ij}^e of micro-elements in a heterogeneous granular system. The fluctuations are complicated in nature and difficult to model. Strain fluctuations for granular material without consideration of polar strain has been studied using Self-consistent method (Chang et.al. 1992) and using method of Distributive tensor (Chang 1993). It is noted that we will evaluate the method of Distributive tensor in detail for predicting the mechanical behavior of heterogeneous granular material in Chapter 3. In trade off complicate analyses, it is desirable to conduct simple analyses for obtaining approximate solutions. In some situations, the results of simple analyses involve straight forward and tractable assumptions which may be more useful in providing insights on the nature of fluctuation of local stress and strain. Although the results of simple analyses are approximate to the exact solutions, they provide bounds and estimates which are useful for assessing the range of mechanical behavior for the complex granular systems. To this end, we conduct analyses with the following four simple assumptions: (For clarity in the subsequent presentation, we drop the subscript for expressions of stress, strain and stiffness tensors.)

(1) uniform strain (i.e., ϵ, γ are constants for all micro-elements)

(2) uniform stress (i.e., σ, μ are constants for all micro-elements)

(3) uniform strain and uniform polar stress (i.e., ϵ, μ are constants for all micro-elements)

(4) uniform stress and uniform polar strain (i.e., σ, γ are constants for all micro-elements)

17

Clearly, the uniform strain assumption of case (1) leads to an upper bound solution, the uniform stress assumption of case (2) leads to a lower bound solution, the partial uniform strain or stress assumptions (i.e., cases (3) and (4)) lead to intermediate solutions. The overall stiffness tensor can then be derived based on the four assumptions, as follows:

Case (1) - uniform strain assumption (ϵ, γ are constants): The effective macro-scale stiffness tensor is the volume average of stiffness tensor for all micro-elements, given by

$$C^{\textit{ff}} = \overline{C} = \frac{1}{V}\sum_e V^e C^e \tag{2.44}$$

where the overline is defined as volume average of local quantities. This definition of overline applies throughout this section.

Case (2) - uniform stress assumption (σ, μ are constants): Inverse of the effective macro-scale stiffness tensor is the volume average of the inverse of stiffness tensor for all micro-elements, given by:

$$C^{\textit{ff}} = \left(\overline{C^{-1}}\right)^{-1} = \left(\frac{1}{V}\sum_e V^e (C^e)^{-1}\right)^{-1} \tag{2.45}$$

where the overline of $\overline{C^{-1}}$ is defined as the volume average of the inversed local stiffness.

Case (3) - uniform strain and uniform polar stress assumption (ϵ, μ are constants): The effective stiffness tensor is given by:

$$C^{\textit{ff}} = \begin{bmatrix} \left(\overline{A^{-1}}\right)^{-1} & \left(\overline{A^{-1}}\right)^{-1}\overline{A^{-1}B} \\ \overline{DA^{-1}}\left(\overline{A^{-1}}\right)^{-1} & \overline{DA^{-1}}\left(\overline{A^{-1}}\right)^{-1}\overline{A^{-1}B} + \overline{E - DA^{-1}B} \end{bmatrix} \tag{2.46}$$

where the overline of $\overline{A^{-1}}$ is defined as the volume average of the inversed local stiffness A^e.

The expressions of A^e, B^e, D^e and E^e can be found in Eq. 2.41.

Case (4) - uniform stress and uniform polar strain assumption (σ, γ are constants): The effective stiffness tensor is given by:

$$C^{\textit{ff}} = \begin{bmatrix} \overline{A - BE^{-1}D} + \overline{BE^{-1}}\left(\overline{E^{-1}}\right)^{-1}\overline{E^{-1}D} & \overline{BE^{-1}}\left(\overline{E^{-1}}\right)^{-1} \\ \left(\overline{E^{-1}}\right)^{-1}\overline{E^{-1}D} & \left(\overline{E^{-1}}\right)^{-1} \end{bmatrix} \tag{2.47}$$

2.5 MODEL PERFORMANCE

To evaluate the applicability of the derived micromechanical model with Delaunay tessellation characterization, we study elastic stress-strain behavior of a random packing of planar disks. The predicted results are compared with the computer simulation results.

A periodic space of randomly packed particles used in this study is shown in Fig. 2.6.

18

The periodic packing can be repetitively stacked to fill the entire space, thus is a representative volume of the granular material. The packing is composed of 1200 particles of radius 0.175 mm and 800 particles of radius 0.100 mm. The total number of contacts in the packing is 5330. The coordination number (the average number of contacts per particle) is 5.33, the area of the representative volume is 174 mm^2 and the void ratio is 0.234.

Mechanical behavior of the packing is obtained from a computer simulation method using the discrete element method by Chang and Misra (1989a). The packing is divided into 2000 Voronoi cells shown in Fig. 2.7 and divided into 4070 Delaunay cells shown in Fig. 2.8. The predicted results obtained from the present model using Delaunay tessellation method are first compared with the computer simulation results and then compared with the results obtained from Voronoi tessellation method.

2.5.1 Comparison with Computer Simulation

To illustrate the heterogeneous nature of strain and stress in the granular system, the variation of these quantities are investigated at the local level. The loading condition is taken to be pure shear. The overall stress and strain for the representative volume are specified to be: $\varepsilon_{11} = 0.22\%$, $\varepsilon_{22} = -0.22\%$, $\sigma_{(12)} = 0$, $\sigma_{[12]} = 0$, $\mu_{13} = 0$, and $\mu_{23} = 0$. The overall stress and strain for the representative volume to be computed are: σ_{11}, σ_{22}, $\varepsilon_{(12)}$, $\varepsilon_{[12]}$, γ_{13}, and γ_{23}. Also computed in the model are the local stress and local strain for each micro-element. The inter-particle stiffness are assumed to be same for all inter-particle contacts, $k_n = 50$ kN/m, $k_s = 40$ kN/m, and $g_s = 0$. The material of concerned is composed of round particles with no rotational resistance.

We list the overall stresses and strains for the representative volume in Table 2.2 and the standard deviation of local stresses and local strains for micro-elements in Table 2.3, predicted under the four different assumptions of heterogeneous states. The results from computer simulation are also listed for comparison. According to Tables 2.2 and 2.3, the results based on the assumptions of uniform polar strain (cases 1 and 3) are in good agreement with those from the computer simulation. However, the results based on the assumptions of uniform polar stress (cases 2 and 4) deviate greatly with those from the computer simulation. Therefore, the assumption of uniform polar strain seems to be better for granular material.

The predicted effective moduli are compared with those obtained from computer simulation to evaluate the micromechanical method. Figures 2.9 and 2.10 show the shear and bulk moduli with different ratio of inter-particle stiffness k_s/k_n, under four different assumptions of the heterogeneous state of the granular packing. In this prediction, for all inter-particle contacts, the normal inter-particle stiffness $k_n = 50$ kN/m, while tangential inter-particle stiffness k_s is chosen as 0, 10, 20, 30, 40, and 50 kN/m. In both Figures, case 1 is the upper bound

19

solution and case 4 is the lower bound solution. Case 2 with uniform polar stress does not give good agreement, in which, the value of k_s has little effect on moduli. The results based on the assumptions of uniform polar strain (cases 1 and 3) provide a good range for upper and lower estimates respectively.

2.5.2 Comparison with Voronoi Tessellation Method

The predicted effective moduli based on Delaunay tessellation method are compared with those based on Voronoi tessellation method. Figures 2.11 and 2.12 show the shear and bulk moduli with different ratio of inter-particle stiffness k_s/k_n. In both figures, the predicted moduli based on Delaunay tessellation method are identical with those predicted based on Voronoi tessellation method for case 1 while the predicted moduli based on Delaunay tessellation method are lower than those predicted based on Voronoi tessellation method for case 3. This is due to the artificial constraint involved in the kinematic assumption in Voronoi tessellation method as described previously. The predicted moduli from case 1 and case 3 for Delaunay tessellation method present a range to cover the computer simulation results.

2.6 Summary

In the micromechanics approach, structure of the granular material can be represented by a set of micro-elements characterized by Delaunay or Voronoi tessellation. We transform the discrete variables of particle translation and particle rotation into continuum variables of strain and polar strain of micro-elements. Correspondingly, we transform the discrete variables of inter-particle force and moment into continuum variables of stress and polar stress.

In a tetrahedral Delaunay cell, the assumption of linear displacement and rotation fields leads to a unique mapping between discrete variables and continuum variables. This uniqueness is not guaranteed for a polyhedral Voronoi cell comprised of more than four faces. Thus linear field assumption used in Voronoi tessellation induces artificial constraints.

The macro-scale constitutive relationship for a representative volume can be derived using four simple assumptions on the fluctuation of micro-element stress and micro-element strain. Based on the example packing, the assumption of uniform polar strain of the present model gives results comparable with those obtained from computer simulation method. However, uniform polar stress seems not to be a good assumption. With the assumptions of uniform strain and uniform polar strain, the present model provides an upper bound solution. With the assumptions of uniform stress and uniform polar strain, the present model provides a lower estimate solution.

20

Discrete variables:	
Generalized particle displacement $\{U_i^n\}$	Translation $\{u_i^n\}$ Rotation $\{\omega_i^n\}$
Generalized inter-particle displacement $\{D_i^c\}$	Inter-particle displacement $\{\delta_i^c\}$ Inter-particle rotation $\{\theta_i^c\}$
Generalized inter-particle force $\{F_i^c\}$	Inter-particle force $\{f_i^c\}$ Inter-particle moment $\{m_i^c\}$
Inter-particle constitutive equation $\{F_i^c\} = [K_{ij}]\{D_j^c\}$	
Continuum variables:	
Generalized strain $\{E_{ij}^e\}$	Stretch strain $\{\epsilon_{ij}^e\}$ Polar strain $\{\gamma_{ij}^e\}$
Generalized stress $\{S_{ij}^e\}$	Cauchy stress $\{\sigma_{ij}^e\}$ Polar stress $\{\mu_{ij}^e\}$
Constitutive equation $\{S_{ij}^e\} = [C_{ijkl}^e]\{E_{kl}^e\}$	
Note:	
$$[K_{ij}] = \begin{bmatrix} k_{ij} & 0 \\ 0 & g_{ij} \end{bmatrix}$$	
$$[C_{ijkl}^e] = \frac{1}{V^e} \sum_c \frac{1}{\alpha^c} [L_{mij}^c]^T [K_{mn}] [L_{nkl}^c]$$	
$$[L_{ijk}^c] = \begin{bmatrix} \delta_{ik} l_j^c & e_{ikl}(X_j^m r_l^{mc} - X_j^n r_l^{nc}) \\ 0 & \delta_{ik} l_j^c \end{bmatrix}$$	

Table 2.1　　Summary of the discrete variables, the continuum variables, and their relationships for a Delaunay micro-element

21

	Computer simulation	ϵ, γ as constants	ϵ, μ as constants	σ, γ as constants	σ, μ as constants
σ_{11} (kPa)	13.743	15.751	8.684	13.236	0.001
σ_{22} (kPa)	-13.537	-15.560	-8.488	-13.163	-0.000
$\sigma_{(12)}$ (kPa)	0	0	0	0	0
$\sigma_{[12]}$ (kPa)	0	0	0	0	0
μ_{13} (kPa-m)	0	0	0	0	0
μ_{23} (kPa-m)	0	0	0	0	0
ϵ_{11} (%)	0.22	0.22	0.22	0.22	0.22
ϵ_{22} (%)	-0.22	-0.22	-0.22	-0.22	-0.22
$\epsilon_{(12)}$ (%)	0.003	0.001	-0.002	-0.002	0.131
$\epsilon_{[12]}$ (%)	0.024	-0.001	0.001	0.001	0.045
γ_{13} (rad/m)	0.023	0.091	-0.380	-0.124	6.242
γ_{23} (rad/m)	0.030	-0.033	0.004	-0.289	10.051

Table 2.2 Predicted overall stresses and strains for the representative volume

	Computer simulation	ϵ, γ as constants	ϵ, μ as constants	σ, γ as constants	σ, μ as constants
σ_{11} (kPa)	3.151	5.835	0.000	0	0
σ_{22} (kPa)	3.091	5.527	0.000	0	0
$\sigma_{(12)}$ (kPa)	1.456	0.404	0.000	0	0
$\sigma_{[12]}$ (kPa)	3.641	3.151	0.000	0	0
μ_{13} (kPa-m)	0.098	0.104	0	0.106	0
μ_{23} (kPa-m)	0.099	0.105	0	0.105	0
ϵ_{11} (%)	0.039	0	0	0.088	1.834
ϵ_{22} (%)	0.038	0	0	0.091	2.257
$\epsilon_{(12)}$ (%)	0.024	0	0	0.014	1.119
$\epsilon_{[12]}$ (%)	0.048	0	0	0.052	0.345
γ_{13} (rad/m)	0.603	0	0.037	0	142.0
γ_{23} (rad/m)	0.721	0	0.054	0	232.0

Table 2.3   Predicted standard deviations of local stresses and local strains for Delaunay micro-elements
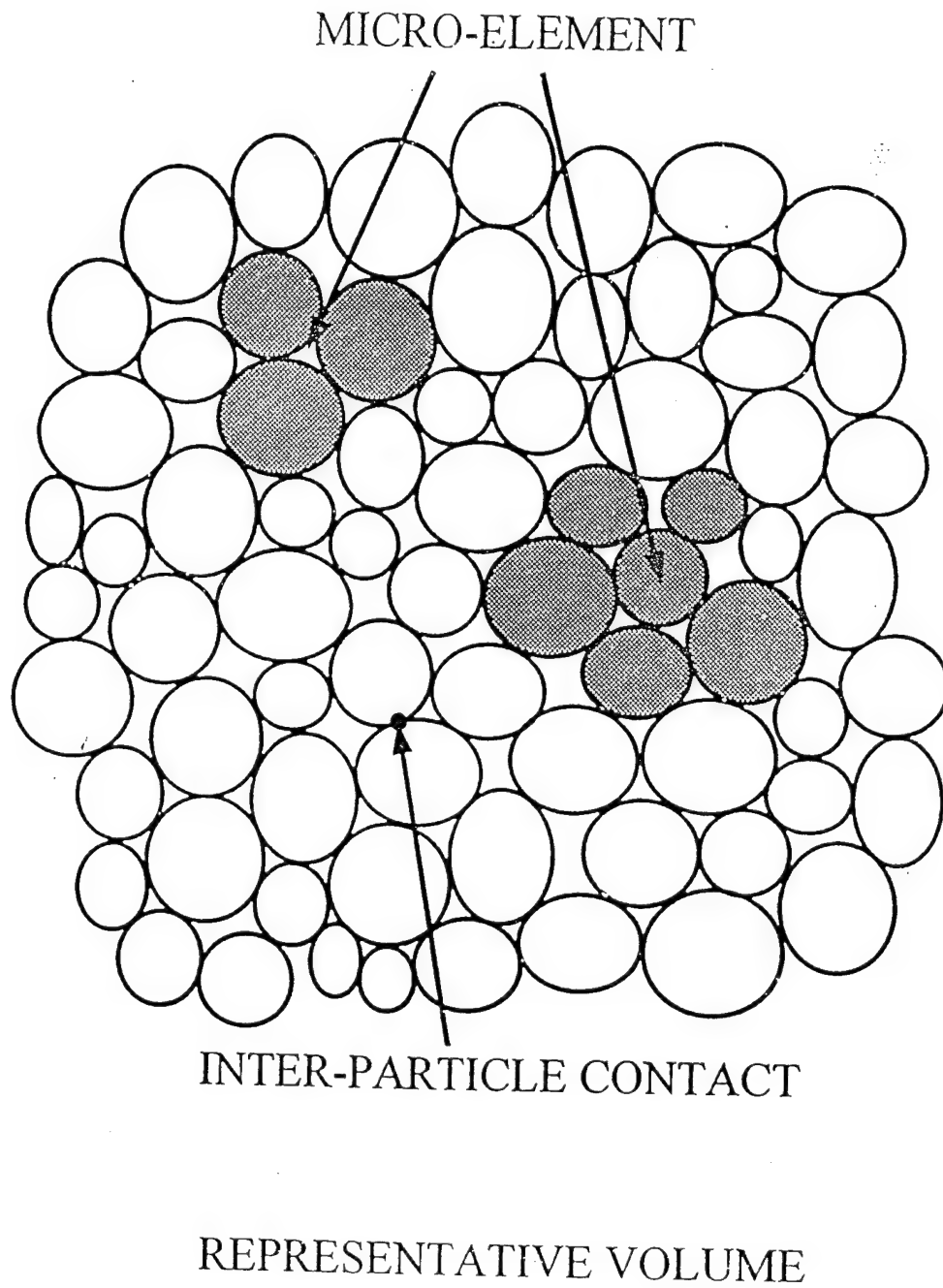
Figure 2.1 Schematic figure for three levels of granular materials
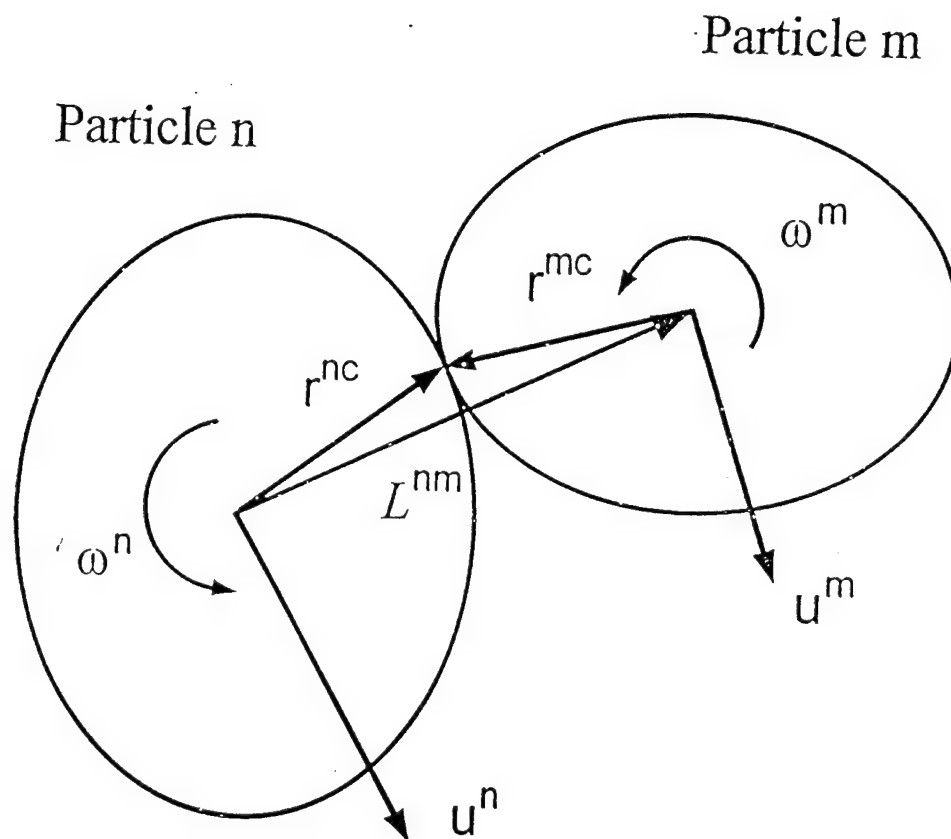
Figure 2.2 Kinematics of two interacting particles

(a)
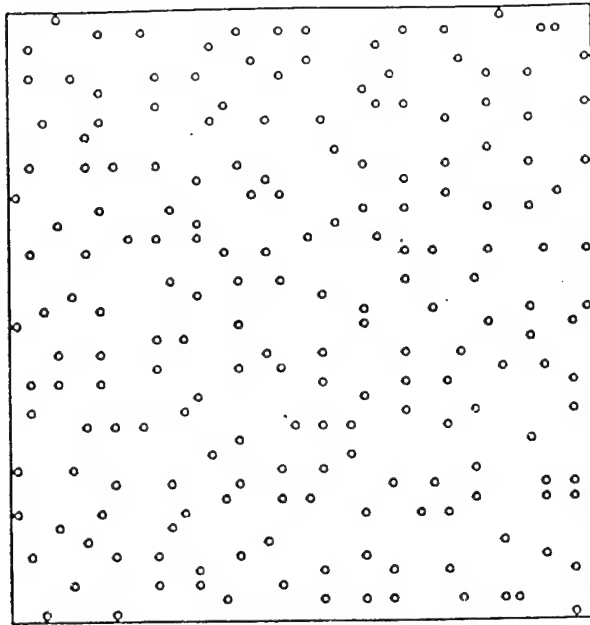
(b)
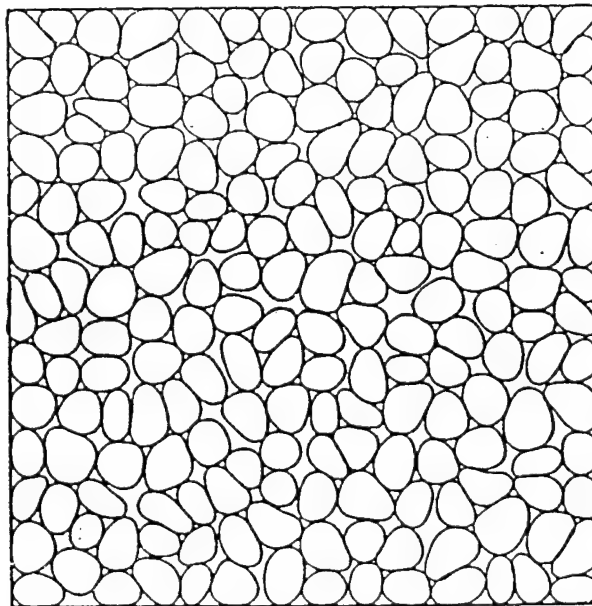
Figure 2.3 (a) random distribution of discrete points; (b) packing of granular particles
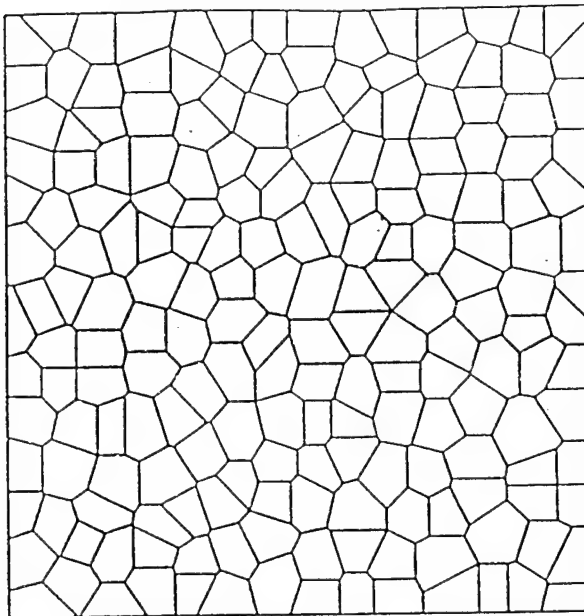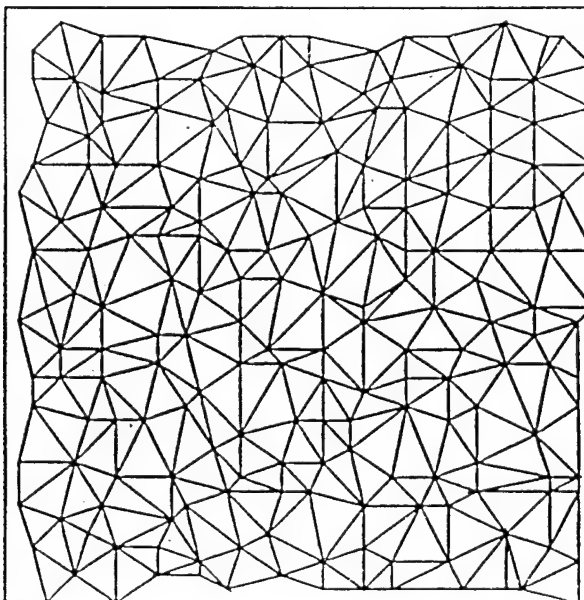
Figure 2.4   Microstructure characterization: (a) Voronoi tessellation; (b) Delaunay tessellation

Micro-element
constitutive law

Micro-element
Stress

Eq. 2.38

Micro-element
Strain

Eq. 2.35

Static
relationship

Eq. 2.26

Kinematic
relationship

Inter-particle
Force

Eq. 2.9

Inter-particle
Displacement

Inter-particle
constitutive law
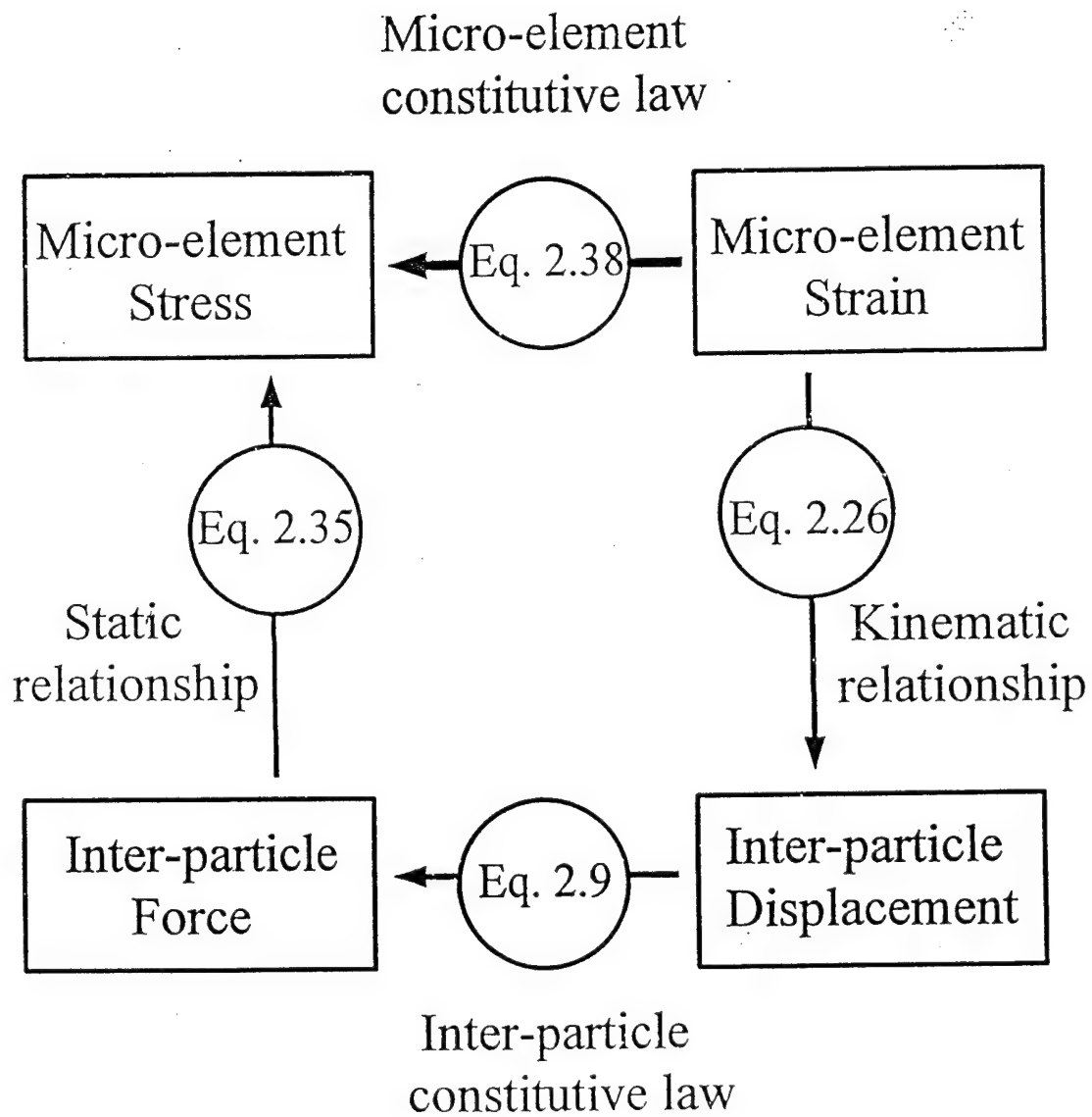
Figure 2.5   Relationships between kinematic and static variables for a Delaunay
micro-element

28
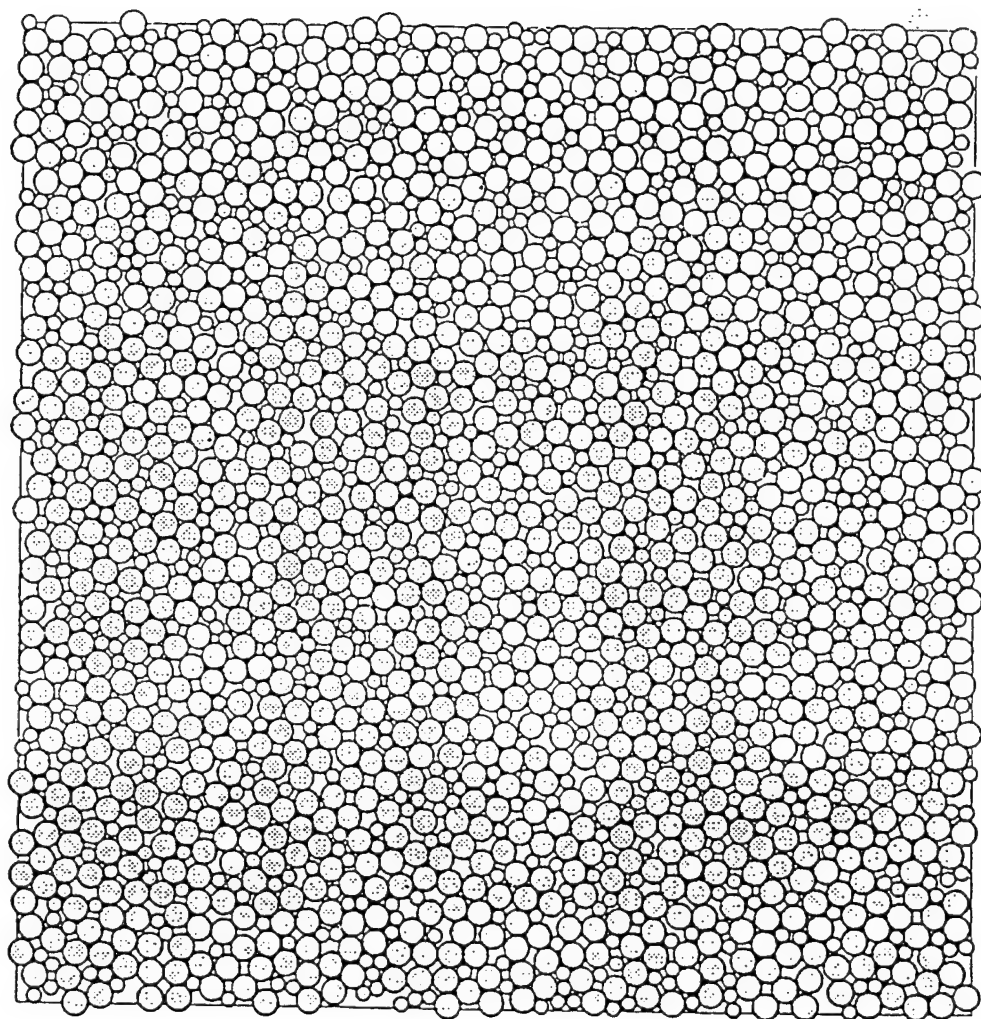
Figure 2.6 Packing structure of the disk assembly used in example
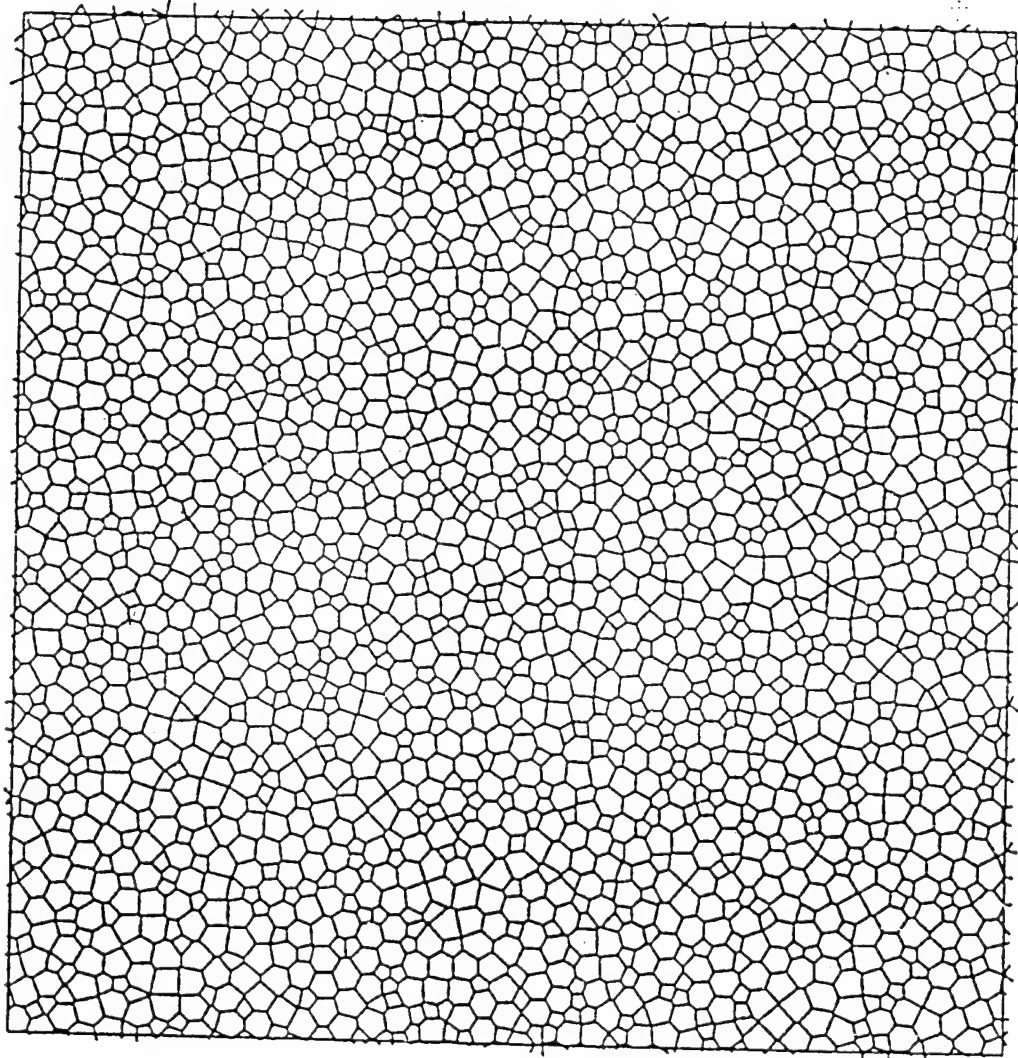
Figure 2.7 Voronoi tessellation of the disk assembly

30
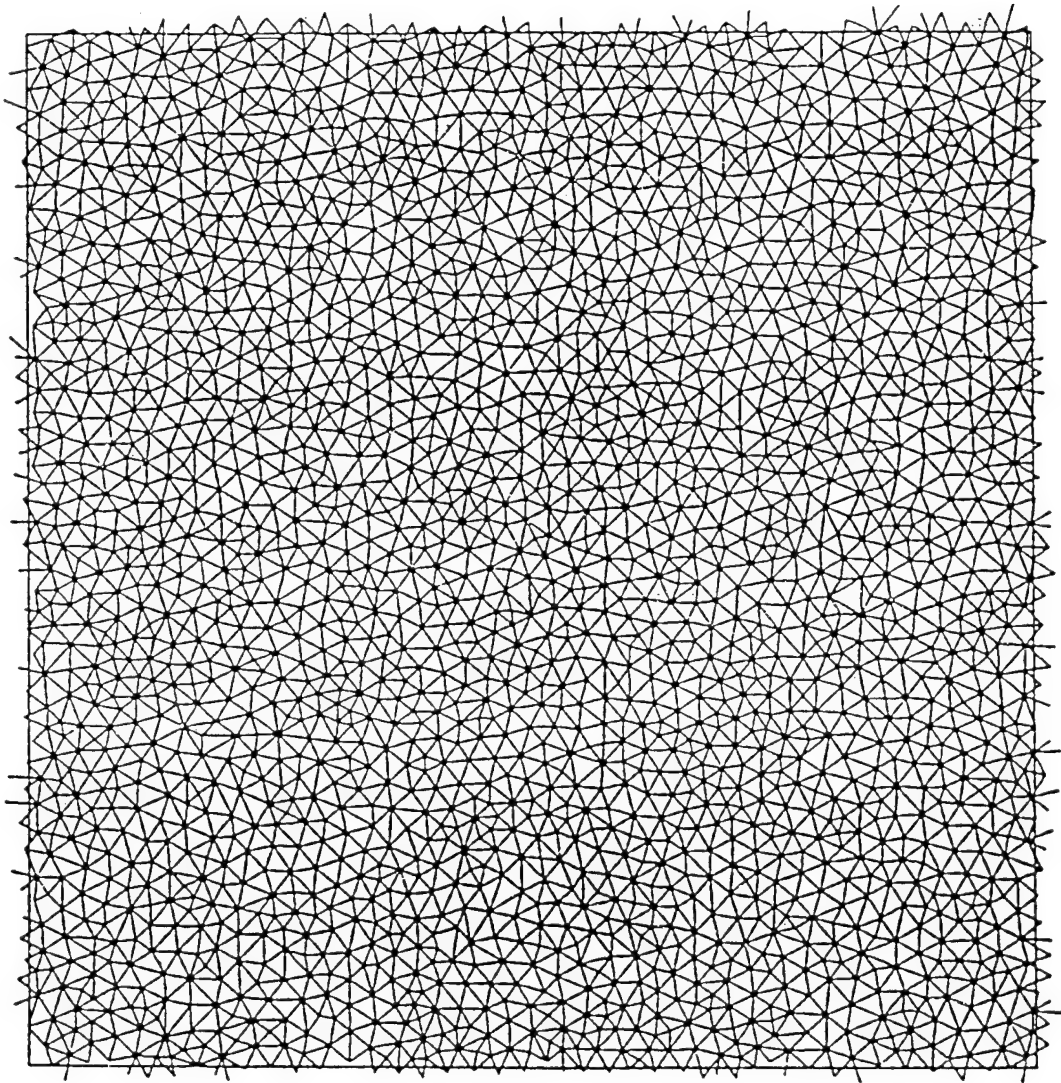
Figure 2.8 Delaunay tessellation of the disk assembly
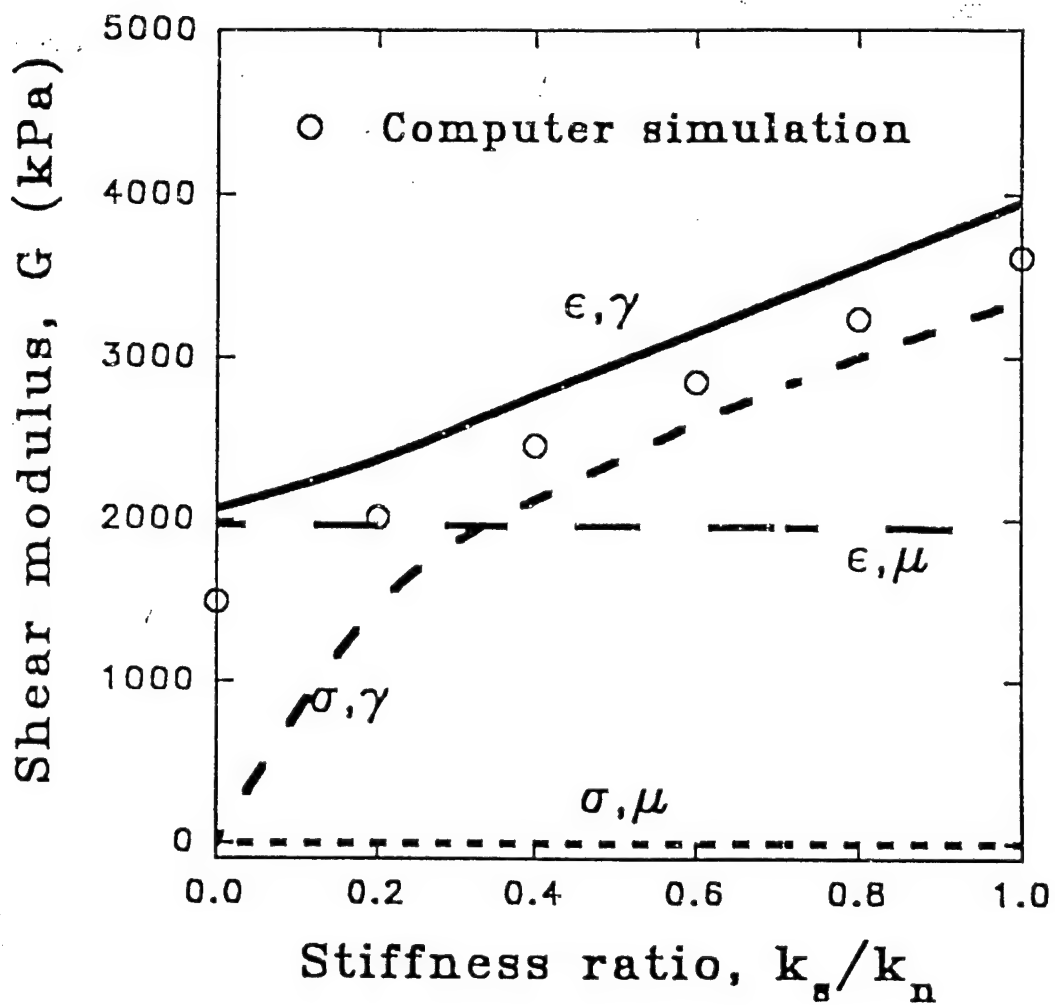
Figure 2.9 Predicted effective shear moduli using the Delaunay tessellation method under four different assumptions
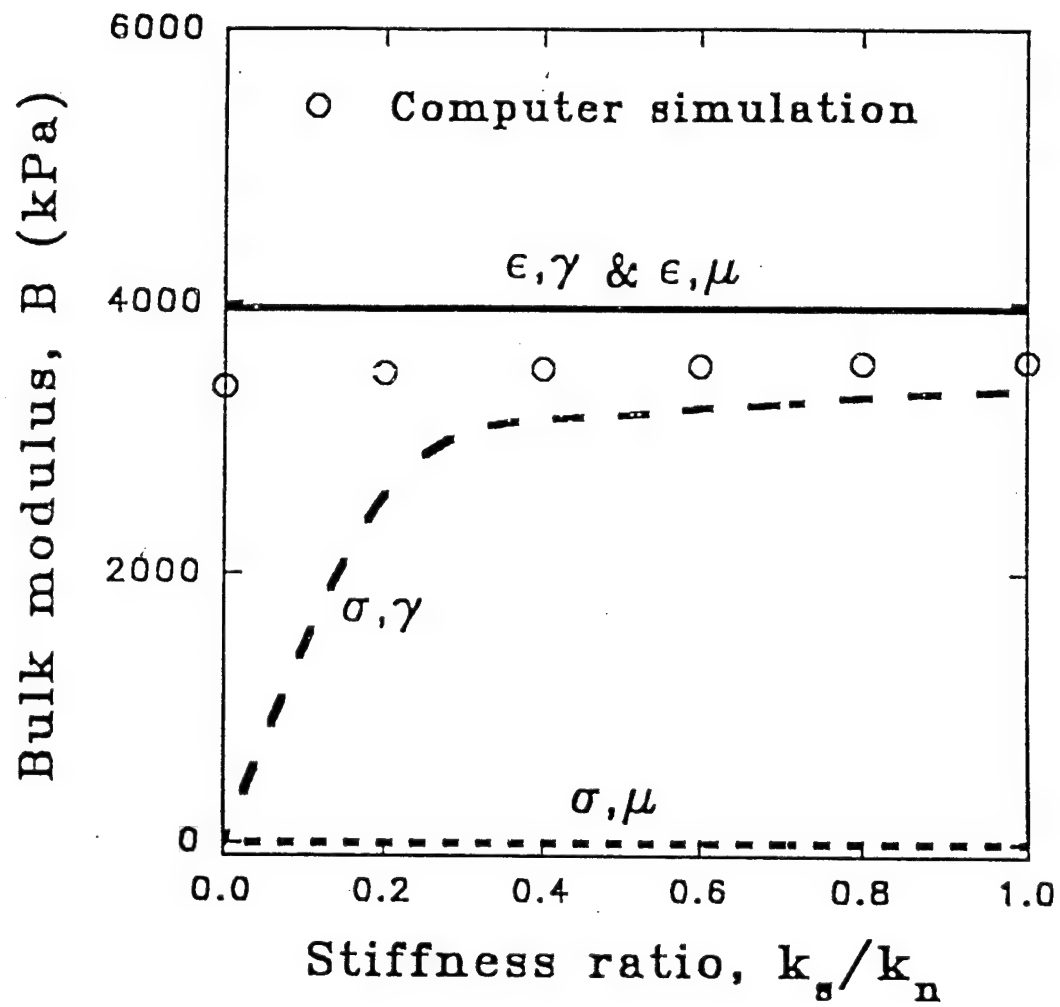
Figure 2.10 Predicted effective bulk moduli using the Delaunay tessellation method under four different assumptions
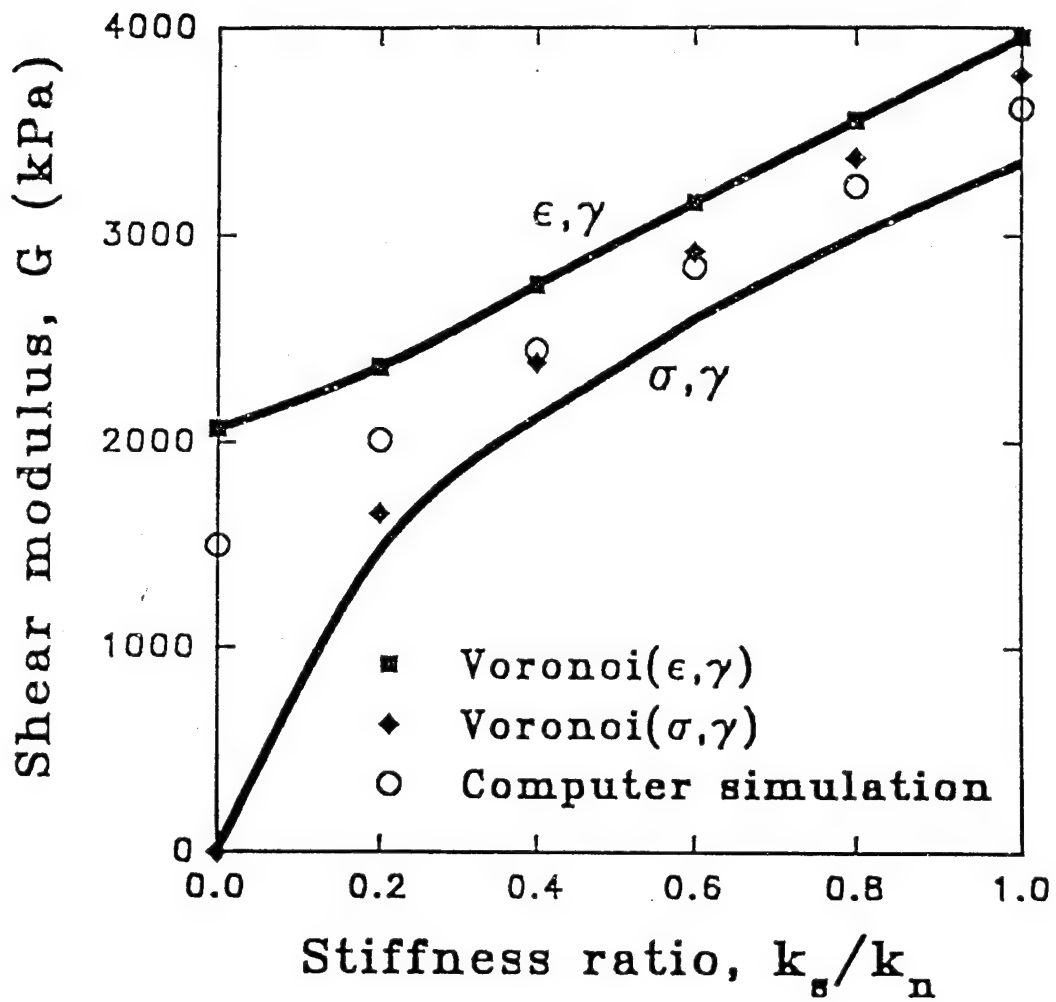
Figure 2.11 Comparison of effective shear moduli predicted by methods based on Voronoi tessellation and Delaunay tessellation
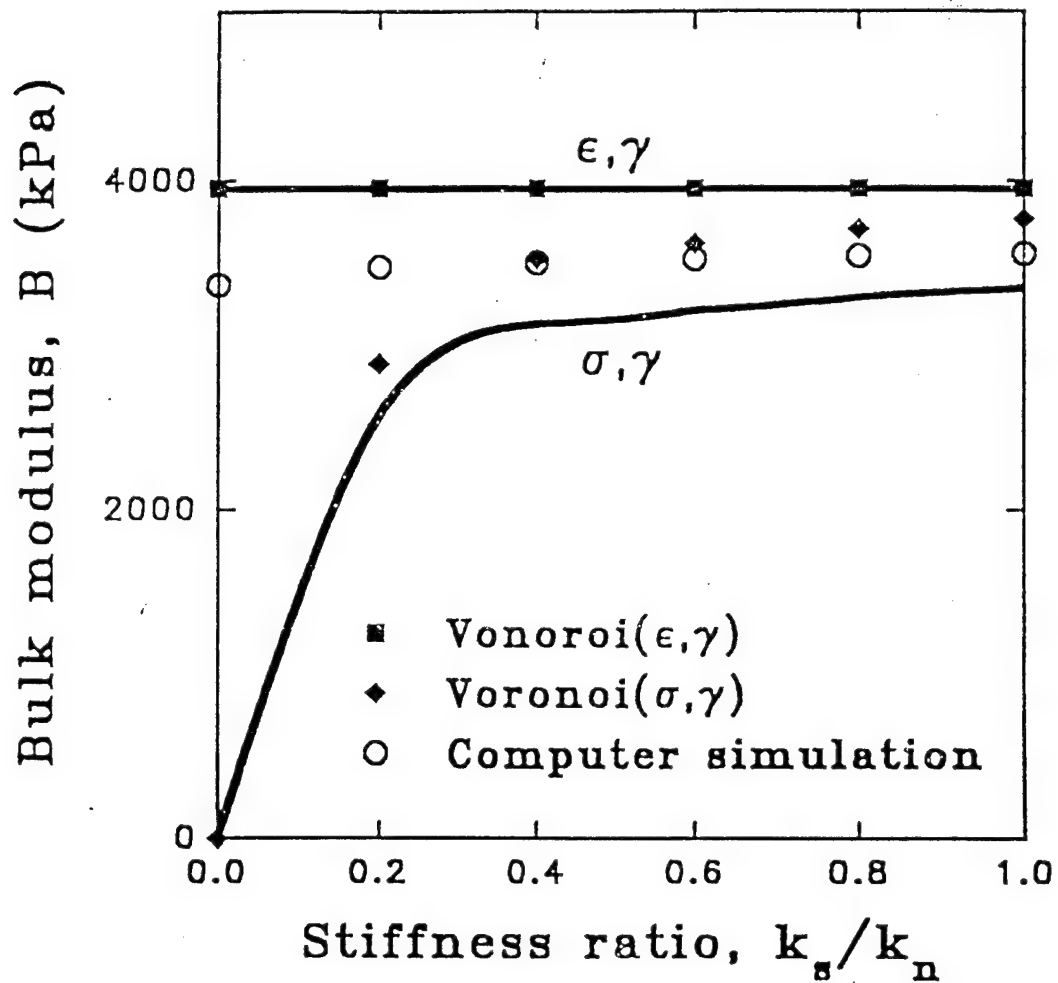
Figure 2.12 Comparison of effective bulk moduli predicted by methods based on Voronoi tessellation and Delaunay tessellation

CHAPTER 3
CLASSES OF EQUIVALENT CONTINUA FOR
GRANULAR MATERIALS

It is desirable to describe the deformation behavior of granular materials using continuum variables such as strain and stress. However the micro scale deformation, attributed to the relative movements of discrete particles, is not a continuous field. Therefore, for the purpose of analysis, it is a fundamental step to transform the discrete particle system to an equivalent continuum system. Choice of the transformation methods results to different types of equivalent of continuum. This chapter describes different classes of continuum which are suitable for representing granular media. More complex continua capture more features of the deformation behavior for granular material. The continua of micropolar type reflect the mechanism of moment transmitting in granular media while the high-gradient continua capture the effect of particle size on wave dispersion.

3.1 INTRODUCTION

Granular material, such as soil, powder, ceramic material, etc., can be perceived as a collection of particles. The overall mechanical properties for granular materials depend significantly on the micro-scale geometric arrangement and on the contact stiffness between two interacting particles. Therefore the effects of particle interaction should be considered in the construction of a mathematical model. However, a granular system is so intricate in its details so as to become essentially intractable. Predictions of each particle movement are costly to extract and usually contain information well in excess of one's needs. It is therefore desirable to transform a discrete particle systems into an equivalent continuum system. The deformation behavior of the granular material is described using suitable continuum variables instead of the movement of individual particles. Granted, the continuum variables can be used to retrieve and keep track the movement of each discrete particles, at least in an approximate manner. This approach allows the construction of a macro-scale constitutive relations for the equivalent continuum of granular materials. The constitutive relations of continuum type is capable of reflecting the discrete nature of particle interaction at micro-scale level.

A number of studies have been attempted along this line of approach. For example, stress-strain relationship was modelled for regularly packed elastic spheres by Deresiewicz (1958), Duffy (1959), Duffy and Mindlin (1957), and more recently, for randomly packed

granules, by Koenders (1987, 1994), Cambou (1993), Bathurst and Rothenberg (1988), Chang (1988), Jenkins (1988, 1993), Walton (1987), etc. These stress-strain models treat the granular material as the traditional continuum in solid mechanics. The stress-strain relationship defined for an infenitesimal element in solid mechanics is now defined for a representative unit cell of the granular media. Since the representative unit cell must contain a large number of particles to be representative of the material, the cell is of finite volume and the stress and strain actually fluctuate within the representative unit cell. Thus the so called stress-strain relationship are referred to the average stress and average strain of the unit cell.

To describe in more detail on the deformation of a representative unit, it is necessary to include suitable continuum descriptors other than stress and strain. For example, with the consideration of particle rotation gradients, the equivalent continuum resembles the continua of micro-polar or Cosserat type (Chang and Liao 1990, Chang and Ma 1991, 1992). Corresponding to the rotation gradients, moments are capable to transmit through the granular medium, which represents a mechanism that can not be modelled by the traditional simple continuum. The effect of moment transmitting becomes important for particle assemblies with cemented inter-particle contacts or with angular particles where the magnitudes of moment transmitted through contacts are significant (Chang and Ma 1992).

With the consideration of higher orders of displacement gradients, the equivalent continuum resembles the continua of high-gradient or non-local type. The use of higher orders of displacement gradients reflects the effect of particle size on the propagating velocities of waves through granular media (Chang and Gao 1995b), which is significant for granular medium with large particle sizes (or short wave lengths). This dispersion phenomenon of wave can not be portrayed by the traditional simple continuum. Elucidated from the recent studies in high gradient models for metals (Coleman and Hodgdon 1985, Triantafyllidis and Aifantis 1986, Bazant and Pijandier-Cabot 1987, Bardenhagen and Triantafyllidis 1994), the model may also be useful in the study of localized deformation associated with shear band for granular media.

In this chapter, we first represent the displacement and rotation fields by continuous polynomial functions. Based on the two continuous fields, we describe different classes of equivalent continua. To illustrate the relationship between micro-macro properties such as internal length of granular material and inter-particle stiffness, we discuss the constitutive constants of a high-gradient model for isotropic granular materials. Example is also given to show the links between the high-gradient model and nonlocal model.

3.2 KINEMATIC DESCRIPTION OF GRANULAR MATERIAL

A simple conceptual model for granular material is to treat it as a collection of particles. When a representative volume element of particles is subjected to an increment of load,

particles undergo translations u_i^n and rotations ω_i^n, resulting in the relative deformation between particles. Based on the kinematics of two particles, the inter-particle displacement and rotation due to relative movement of two particles generate inter-particle forces and inter-particle moments in granular materials. The magnitudes of forces and moments depend on the contact stiffnesses.

For two identical elastic spherical particles in contact, the contact area is of circular shape, values of contact stiffness can be obtained from Hertz-Mindlin contact theory as a function of particle properties and contact force. While the translational contact stiffness are responsible for transmitting forces through inter-particle contacts, the rotational contact stiffness are responsible for transmitting moments through inter-particle contacts in a granular media.

To develop a continuum mechanics model for the behavior of particle assembly, it is desirable to view the discrete system as an equivalent continuum system. To this end, we define the displacement and rotation of discrete particles as macro-scale continuum fields, denoted as: displacement $u_i(x)$ and rotation $\omega_i(x)$. When x is located at the centroid of n-th particle, the functions represent the displacement and rotation of the n-th particle,

$$u_i(x_i^n) = u_i^n$$
$$\omega_i(x_i^n) = \omega_i^n$$

(3.1)

Following the approach by Chang and Liao (1990) using polynomial expansion for the displacement and rotation fields, the displacement and rotation of the m-th particle can be estimated from the deformation gradients at the neighbouring n-th particle, given by

$$u_i^m = u_i^n + u_{i,j}^n L_j^{nm} + \frac{1}{2} u_{i,jk}^n L_j^{nm} L_k^{nm} + \ldots\ldots$$
$$\omega_i^m = \omega_i^n + \omega_{i,j}^n L_j^{nm} + \frac{1}{2} \omega_{i,jk}^n L_j^{nm} L_k^{nm} + \ldots\ldots$$

(3.2)

where the branch vector $L_i^{nm} = r_i^{nc} - r_i^{mc}$; the displacement and rotation derivatives of the n-th particle are treated to be the continuum kinematic variables.

It is noted that the rotation and displacement are not two independent variables. During deformation of a granular material, the rotation of a particle consists of two

38

components: the rigid body rotation and the particle spin. While the particle spin is independent of the displacement field, the rigid body rotation is solely induced by the displacement field from the skew-symmetric part of displacement gradients.

3.3 DIFFERENT CLASSES OF CONTINUA

The discrete system can be characterized as an equivalent continuum system based on the two continuous fields of displacement and rotation. The discrete variables and the continuum variables are linked through the series expression of Eq. 3.2. When the number of terms in this series is large enough, the continuum system can capture as much details as the discrete system. A simplified kinematic description leads to a simpler continuum model for the discrete system while still capturing the essential features of granular materials.

Different degrees of approximation of Eq. 3.2 lead to different classes of 'continua'. We classify the models into categories: (1) high gradient continua - including higher orders of deformation gradients, and (2) first gradient continua - including only the first order of deformation gradients.

High Gradient Continua

Class 1 : High Gradient Micro-polar Continua

Particle spin and moment transmitting through the continua are considered. The continuum variables involves higher orders of both displacement and rotation gradients.

Class 2 : High Gradient Couple stress / Cosserat Continua

The particle spin is neglected, thus the particle rotation is induced solely from the rigid body rotation of displacement field. The gradients of rigid body rotation can still cause the transmitting of contact moments through granular material. This mechanism resembles that proposed in couple stress theory and Cosserat theory (Cosserat 1909, Truesdell and Toupin 1960, Toupin 1962, Mindlin and Tiersten 1962). The moment transmitting are found to have interesting effects on the propagation and dispersion of waves in granular media (Chang and Gao 1995b).

Class 3 : High Gradient Non-polar Continua

Same as class 2, we further neglect the moment transmitting caused by the gradients of rigid body rotation. The continuum variables still involves higher orders of displacement gradients. Chang and Gao (1995a) have derived this class of constitutive models for granular materials.

First Gradient Continua

Class 4 : Micro-polar Continua

Using up to the first-order gradients of displacement and rotation. The continua resemble the micro-polar type proposed by Eringen (1968). Constitutive law of this type for granular material shows that moment trasmitting can effect significantly the stress distribution under loads (Chang and Ma 1991, 1992).

Class 5 - Quasi Micro-Polar Continua

Neglecting the particle rotation gradient, the particles within a group of particles spin with the same magnitude. In this situation, the granular medium does not transmit moment thus is no longer a micro-polar medium. However, since the particle spin is still in presence, the granular medium is of a quasi-micropolar type. Chang and Misra (1989) and Chang (1993) have derived this class of constitutive models for granular materials.

Class 6 : Classic Continua

With further neglect of the particle spin from class 5, the particle rotation is identical to the rigid body rotation. Constitutive law for granular medium thus derived resembles that of classic continua in solid mechanics. Constitutive models of this class for granular material can be found in the work by Bathurst and Rothenberg (1988), Chang (1988), Jenkins (1988), Walton (1987), etc..

Most work in the literature on micro-macro properties of granular material treat granular material as first gradient continua in the classes 4-6. Due to the difficulties of dealing with the high-rank tensors, very little attention has been paid to the representation of granular material as high gradient continua in the classes 1-3. To illustrate the relationship between micro-macro properties such as internal length of granular material and inter-particle stiffness, we discuss the constitutive constants of a high-gradient model for isotropic granular materials.

3.4 CONSTITUTIVE RELATIONSHIP FOR AN ASSEMBLY

For a representative volume of the granular material, the medium can be treated as statistically homogeneous and can thus be regarded as centrical symmetry. Under this situation, the effect of the first gradient of strain and rotation can be neglected and the constitutive equation for the granular assembly is in the following form

$$\sigma_{ij} = A_{ijkl}e_{kl} + B_{ijklmn}e_{kl,mn} + E_{ijklmn}u_{[k,l],mn} \tag{3.3}$$

40

This type of high-gradient constitutive law for granular material is in the same class of constitutive law proposed by Toupin and Gazis (1964), Mindlin (1965), Coleman and Hodgdon (1985), etc.

Consider an idealized granular material which is made of equal-size spheres with an isotropic packing structure; The material has identical inter-particle stiffness for all contacts which is independent of contact force. The expression of constitutive relation is given by (Chang and Gao 1995a)

$$\sigma_{(ij)} = \lambda \delta_{ij} \varepsilon_{kk} + 2\mu \varepsilon_{ij}$$
$$+ C_1 \delta_{ij} \nabla^2 \varepsilon_{kk} + C_2 (\nabla^2 \varepsilon_{ij} + \varepsilon_{kk,ij})$$

(3.4)

In this equation, λ and μ are the Lame constants which relate to the inter-particle stiffness by

$$\lambda = 4\alpha(K_n - K_s)$$
$$\mu = 2\alpha(2K_n + 3K_s)$$

(3.5)

where $\alpha = \dfrac{Mr^2}{15V}$ represents the density of packing structure. M is the total number of inter-particle contacts in the representative volume V, and r is the radius of particles. The other two constants corresponding to the high-gradient terms are as follows:

$$C_1 = \frac{8}{7}\alpha r^2 (K_n - K_s)$$
$$C_2 = \frac{16}{7}\alpha r^2 (K_n + \frac{3}{4}K_s)$$

(3.6)

3.4.1 Micro-macro Properties

Compare the derived stress-strain law with generalized Hooke's law, the constants λ

and μ are the usual Lame constants. The corresponding Young's modulus and Poisson's

ratio are derived as:

This equation provides a method for estimating elastic moduli based on the values of inter-particle stiffness. Eq. 3.5 can also be rearranged, given by

41

$$E = \frac{4Mr^2}{3V}\left(\frac{2K_n + 3K_s}{4K_n + K_s}\right)$$

$$\nu = \frac{K_n - K_s}{4K_n + K_s}$$
(3.7)

$$K_n = \frac{3\lambda + 2\mu}{20\alpha}$$

$$K_s = \frac{\mu - \lambda}{10\alpha}$$
(3.8)

which provides a means for estimating inter-particle stiffness based on the measured value of elastic moduli.

The values of high gradient constitutive coefficients C_1 and C_2 are expressed in terms of contact stiffness as given in Eq. 3.6. Substituting Eq. 3.8 into Eq. 3.6, the values of C_1 and C_2 can be expressed in terms of Lame constants as follows:

$$C_1 = \frac{2}{7}\lambda r^2$$

$$C_2 = \frac{4}{7}\mu r^2\left(1 + \frac{3(\lambda - \mu)}{10\mu}\right) ; \quad \text{or} \quad C_2 = \frac{2}{35}\mu r^2\left(\frac{7 - 8\nu}{1 - 2\nu}\right)$$
(3.9)

Eq. 3.9 provides a useful method for estimating the high gradient constitutive constants, C_1, C_2 , directly from the Lame constants and particle size. This relationship is of practical use since the high gradient constitutive coefficients are difficult to be evaluated from laboratory test.

3.4.2 Role of Internal Length and Inter-particle Stiffness

The high-gradient constitutive constants, C_1, C_2 are functions of internal length r of the granular assembly which represents the particle size. When the particle size of a granular material is very small compared with the representative volume of the material, the effect of strain gradient in the constitutive equation can be neglected. Thus, the constitutive equation reduces to the generalized Hooke's law for granular materials. On the other hand, the effect of strain gradient becomes pronounced as the particle size increases.

42

Inter-particle stiffness have significant effect on the second-gradient constitutive coefficients. Three cases are noted:

(1) K_s/K_n is less than 1: This corresponds to particles with smooth surface. Such a ratio of inter-particle stiffness leads to a positive Poisson's ratio and thus a positive λ and a positive C_1. As the ratio of K_s/K_n decreases (i.e., smoother surface), values of C_1 and λ increase while value of C_2 decreases. The limiting value physically possible for K_s/K_n is zero. Corresponding to this limiting condition, it is noted that, under the present formulations for granular assemblies with spherical particles, the predicted Poisson's ratio can not be greater than 0.25 and the Lame constant λ can not be greater than μ.

(2) K_n/K_s is equal to 1: This corresponds to particles with rough surface. Such a ratio of inter-particle stiffness leads to a zero Poisson's ratio and thus a zero λ and a zero C_1. Under this condition, C_2 is a positive number.

(3) K_s/K_n is greater than 1: This corresponds to particles with very rough surface, which is an unusual situation. Such a ratio of inter-particle stiffness leads to a negative Poisson's ratio and thus a negative λ and a negative C_1.

3.5 COMPARISON WITH OTHER MODELS

A convenient simple form based on the second-gradient theory can be arrived by neglecting the effects of volume strain gradient $\varepsilon_{kk,ij}$ in Eq. 3.4, and by assuming the condition of $K_s = 0$.

43

The simplified version of Eq. 3.4 takes the following form of constitutive equation

$$\sigma_{ij}=(1+c\nabla^2)(\lambda\,\delta_{ij}\varepsilon_{kk}+2\mu\,\varepsilon_{ij}) \tag{3.10}$$

where c is a positive constants, $c=\dfrac{2}{7}r^2$.

It is noted that the simplified model of second- gradient theory (with $K_s = 0$) given in Eq. 3.10 is similar to the form given by Bazant and Pijaudier-Cabot (1989) based on nonlocal continuum theory, and the linear model of Mindlin's second-gradient theory (Mindlin, 1965, Beran and McCoy, 1970b).

Comparison between nonlocal model and high-gradient model for composite media can be found in the work by Beran and McCoy (1970a, b) and Levin (1971). Here we discuss the relations between nonlocal theory and the present high-gradient model for granular material. Based on Taylor's expansion (Eq. 3.2), the high gradients of displacement at the local point 'n' contribute to the displacement at another local point 'm' in the neighbouring distance. Therefore, second-order gradient terms in the present model reflect the effect of neighbouring medium on a local point. It is thus expected the high-gradient model is equivalent to the nonlocal model under certain conditions.

In the Eringen-Kroener model of nonlocal elasticity, the constitutive equation is

$$\sigma_{ij}(x)=\int_V \alpha\left(|x-x'|\right)\left(\lambda\,\delta_{ij}\varepsilon_{kk}(x')+2\mu\,\varepsilon_{ij}(x')\right)dv(x') \tag{3.11}$$

where $\alpha\left(|x-x'|\right)$ is the non-local function (see Kroener, 1967; Eringen and Edelen, 1972; Eringen, 1973). Expand the strain in the integrand at point x, i.e.

$$\varepsilon_{ij}(x')=\varepsilon_{ij}(x)+(x_k'-x_k)\frac{\partial\varepsilon_{ij}(x)}{\partial x_k}+\frac{1}{2}(x_k'-x_k)(x_l'-x_l)\frac{\partial^2\varepsilon_{ij}(x)}{\partial x_k\partial x_l}+... \tag{3.12}$$

and substitute the series of the strain in Eq. 3.12 into Eq. 3.11 of nonlocal model. After neglecting higher terms, we obtain the first-order approximation of nonlocal model, given by

$$\sigma_{ij}=(1+c\nabla^2)(\lambda\,\delta_{ij}\varepsilon_{kk}+2\mu\,\varepsilon_{ij})$$

$$c=\int_V\frac{1}{2}\alpha\left(|x'-x|\right)(x_k'-x_k)^2dv(x') \tag{3.13}$$

in which the integrand of Eq. 3.13 and the resultant c is positive. The value of c depends on

44

the nonlocal function. Note that the first-order approximation of nonlocal model given in Eq. 3.13 is same as the simplified form of the present high-gradient model in Eq. 3.10, and the constant in Eq. 3.13, $c = \frac{2}{7}r^2$.

3.6 SUMMARY

In this chapter, classes of equivalent continua for granular materials are described. As expected, during the transformation from a complicated discrete system to a simpler continuum system, certain information are lost. Therefore, the constitutive relations for the equivalent continuum can not respond, on the macro scale, all deformation features just as the original granular material does. How simple the equivalent continuum should be depends on how much "essential behavior" of the granular materials are of interest. Unfortunately, the limitations of modelling capability are inherited from the type of continuum. Therefore the required modelling capability for problems encountered determines what type of equivalent continuum to be selected for analysis. For example, the continuum of micropolar type is useful to the study of moment transmitting in granular media while the high-gradient continua is useful to the study of particle size effect on wave dispersion.

CHAPTER 4
Wave Propagation in Granular Material
Using High Gradient Theory

Treating granular materials as a high gradient continue media, the propagation of wave in granular materials are analyzed. The constitutive coefficients of the high gradient continue are expressed in explicit functions of inter-particle stiffness. In contrast to the classical continue, the high gradient terms represent the internal characteristic length of granular materials. With the high gradient model, we solve the wave propagation in a finite strip of granular material using the method of separated variables, in which the orthogonal eigenfunctions can be obtained from the boundary conditions. The short waves with lengths less than about two times of the particle diameter can not propagate through the granular material because of the discrete nature of the granular material. The solution derived from the high gradient theory consists of a series of harmonic waves which are admissible of propagation in the granular material. The present numerical results show that due to the nonlinear dispersion of wave in granular medium, the peak value of the stress wave will be decay as wave propagating. A series smaller stress waves including extension and compression waves will be emerge after the main stress wave goes through, which is caused by the reflection of the stress wave on boundary of inter-particles. The predicted phenomena are qualitatively in agreement with the simulation results from discrete element methods and with the experimental observations from a chain of photo-elastic disks subjected to a impact load.

4.1 INTRODUCTION

Dynamic response of granular material, such as soil, ceramic and powder material, has been of interest to the field of civil engineering, material processing and geophysics. This chapter is aimed to study wave propagation in granular material treated as a high gradient media.

The high gradient elastic stress-strain model used in this chapter was developed from a micromechanics approach, in which the constitutive coefficients are expressed as explicit functions of inter-particle stiffness and particle size (C.S. Chang and J. Gao, 1995a,b). In this chapter, the high gradient model is applied to analyze the wave propagation in a finite strip fixed at one end and subjected to dynamical traction at the other. The solution can be

obtained from the solutions of a series of harmonic waves using the method of separation of variables. The solution proves that the short waves with lengths less than about two times of the particle diameter can not propagate through because of the discrete nature of the granular material. The solution also shows a decay of the peak of stress wave as the propagation of the wave. This phenomenon is similar to the decay of peak contact force observed from experiments by A Shukla and C. Damania(1988) and from Discrete Element Analysis by C. Thornton and Randall, C.W.(1988), Sadd etc(1992), J.S. Lee etc(1992), for a chain of disks. This chapter discuss the decay of the peak stress influenced by the size of particles.

In this microstructural continuum model, the stress wave excited by dynamic impact consists of both compression and extension waves propagating along the granular material. This is different from a simple compression wave in classic solution of elastic material. The phenomenon of tension reflection is similar to that from Discrete Element analysis (J.S.Lee etc. 1992). The solution shows that this high gradient continuum model captures important salient features of granular material.

4.2 WAVE PROPAGATION IN A FINITE STRIP OF GRANULAR MATERIALS

Granular material can be treated as a collection of particles. The geometric deformation in discrete system are described by the translations u_i^n and rotations ω_i^n (n=1,2,...). To develop a continuum mechanics model for the behavior of particle assembly, it is desirable to view the discrete system as an equivalent continuum system. To this end, we define the macro-scale continuum geometric deformation fields as: displacement $u_i(x)$ and rotation $\omega_i(x)$. When x is located at the centroid of n-th particle, the continuum geometric fields are compatible with that of the discrete system, i.e. $u_i(x^n) = u_i^n$ and $\omega_i(x^n) = \omega_i^n$. Therefore the inter-particle displacement δ_i^{nm} and inter-particle rotation ω_i^{nm} can be expressed as a series of high gradients of the particle deformations. From the kinematic hypothesis, the constitutive law of granular material with random packing structure can be expressed as follows (C.S. Chang and J. Gao 1995b):

$$\sigma_{ij} = \lambda \delta_{ij} \varepsilon_{kk} + 2\mu \varepsilon_{ij} + C_1 \delta_{ij} \nabla^2 \varepsilon_{kk} + C_2 (\nabla^2 \varepsilon_{ij} + \varepsilon_{kk,ij}) + C_3 \nabla^2 u_{[i,j]} \tag{4.1}$$

where the constitutive constants are dependent of inter-particle properties and the size of particles, given by

47

$$\lambda = 4\alpha(K_n - K_s), \qquad \mu = 2\alpha(2K_n + 3K_s)$$

$$C_1 = \alpha_c(K_n - K_s), \qquad C_2 = 2\alpha_c(K_n + \frac{3}{4}K_s)$$

$$C_3 = 2\alpha(G_n - G_s), \qquad \alpha = M\frac{r^2}{15V}, \quad \alpha_c = \frac{8}{7}\alpha r^2$$

in which M is the total number of inter-particle contacts in the representative volume V; r is the radius of particles; and $[K_n, K_s, G_n, G_s]$ are the distortion and rotation contact stiffness constants along normal and tangential directions respectively.

We now consider the case of wave propagation in a finite strip of granular material. In this case, only the displacement $u(x,t)$ and stress $\sigma(x,t)$ in x-direction are considered. The constitutive equation of stress $\sigma(x,t)$ in the aforementioned high gradient model is given by

$$\sigma(x,t) = (\lambda + \mu)[\frac{\partial u(x,t)}{\partial x} + c\frac{\partial^3 u(x,t)}{\partial^3 x}] \tag{4.2}$$

where $c = \frac{C_1 + 2C_2}{\lambda + 2\mu} = \frac{2}{7}r^2\frac{5K_n + 2K_s}{3K_n + 2K_s}$.

With the high gradient model, the one dimensional wave equation becomes

$$\rho\frac{\partial^2 u}{\partial t^2} = \frac{\partial \sigma}{\partial x} = (\lambda + 2\mu)(1 + c\frac{\partial^2}{\partial x^2})\frac{\partial^2 u}{\partial x^2} \tag{4.3}$$

where ρ is the material mass density.

It is noted that the wave equation is a fourth-order differential equation. When the influence of the internal length on material behavior is neglected, i.e. c=0, the wave equation in Eq. 4.3 reduces to the classical form in elastic-dynamics. The wave-propagation in the finite strip requires four boundary conditions and two initial conditions. Two of the boundary conditions are given by

$$u(0,t) = 0; \qquad \varepsilon(L,t) = \frac{\partial u(L,t)}{\partial x} = \frac{p(t)}{\lambda + 2\mu}; \qquad t > 0 \tag{4.4}$$

The two extra boundary conditions, by use of variational principle, should be

$$\frac{\partial^2 u(0,t)}{\partial x^2} = 0; \quad \frac{\partial^2 u(L,0)}{\partial x^2} = 0 \tag{4.5}$$

or

$$\frac{\partial^2 u(0,t)}{\partial x^2} = 0; \quad \frac{\partial^3 u(L,0)}{\partial x^3} = 0$$

The initial conditions are

$$u(x,0) = u_0(x); \qquad \frac{\partial u(x,t)}{\partial t}\Big|_{t=0} = v_0(x); \qquad 0 < x < L \tag{4.6}$$

In the following, two types of excitation are discussed, namely, initial disturbance and dynamic traction.

4.3 WAVE PROPAGATION SUBJECT TO INITIAL DISTURBANCES

First, we consider that the wave in the finite strip is excited by the initial disturbance which described by the initial conditions Eq. 4.6 with the homogeneous boundary conditions.

To obtain the solution by the method of eigenfunction expansion, we further propose the solution to be in the form $u(x,t) = T(t) X(x)$. Substituting the assumed solution into Eq. 4.3 and separating the variables, we can express the wave equation as two ordinary differential equations, given by

$$\ddot{T}(t) + \omega^2 T(t) = 0$$

$$c X^{IV}(x) + X''(x) + \frac{\omega^2}{V^2} X = 0 \tag{4.7}$$

with the boundary conditions

$$X(0) = 0, \quad X''(0) = 0; \qquad X'(L) = 0, \quad X'''(L) = 0 \tag{4.8}$$

Clearly, the function $\exp(i\omega t)$ is a solution of Eq. 4.7 which corresponds to the harmonic wave propagating in material. The constant ω is the natural frequency of the system. The solution of equation (4.7b) leads to a series of eigenvalues ω_n $(n = 1,2,3,...)$. A particular mode of the oscillation is termed the eigenfunction $X_n(x)$ associated with the natural frequency ω_n . The eigenvalues $\beta = \frac{\omega^2}{V^2}$ satisfy the following theorems:

Theorem 1. All eigenvalues $\beta_n = \frac{\omega_n^2}{V^2}$ of Eq. 4.7 are real when the natural boundary

conditions are satisfied.

Theorem 2. The eigenfunctions associated with real β_n constitute an orthogonal set. ·

49

It is noted that the solution of Eq. 4.7b is dependent on the constitutive parameter of high gradient term.

(a) When $4c\beta > 1$, the solution can be expressed as follows

$$X(x) = \exp(-K_1 x)[A\cos(K_2 x) + B\sin(K_2 x)] + \exp(K_1 x)[C\cos(K_2 x) + D\sin(K_2 x)] \quad (4.9)$$

where $K_1 = \sqrt[4]{\dfrac{\beta}{c}}\sin\dfrac{\theta}{2}$; $K_2 = \sqrt[4]{\dfrac{\beta}{c}}\cos\dfrac{\theta}{2}$.

To satisfy the boundary conditions given by Eq. 4.8, we substitute Eq. 4.9 into Eq. 4.8 leading to a set of linear algebra equations with the coefficients A,B,C and D. It can be seen that non-trivial solution of A, B, C and D can be obtained if and only if the parameter matrix is zero. Since the parameter matrix of the linear equations is not equal to zero, i.e.

$$2K_1 K_2 (K_1^2 + K_2^2)(\cos^2(K_2 L)\,ch^2(K_1 L) + \sin^2(K_2 L)sh^2(K_1 L)) \neq 0 \quad (4.10)$$

Therefore, the constants A = B = C = D = 0.

(b) When $4c\beta \leq 1$, the solution of eigenfunction can be expressed as the following form

$$X(x) = A\cos(\frac{x}{\sqrt{2c}}\sqrt{1+\sqrt{1-4c\beta}}) + B\sin(\frac{x}{\sqrt{2c}}\sqrt{1+\sqrt{1-4c\beta}})$$

$$+ C\cos(\frac{x}{\sqrt{2c}}\sqrt{1-\sqrt{1-4c\beta}}) + D\sin(\frac{x}{\sqrt{2c}}\sqrt{1-\sqrt{1-4c\beta}}) \quad (4.11)$$

From the boundary conditions, we can again obtain the linear algebra equation of the constants A, B,C and D. At $x=0$, the linear algebra equations gives $A=C=0$. Applying the boundary conditions on another end of the strip, it can be seen that non-trivial solution of B and D can be obtained if and only if the parameter matrix is zero, i.e.

$$\cos(\frac{L}{\sqrt{2c}}\sqrt{1+\sqrt{1-4c\beta}}) = 0 \quad (4.12)$$

or

$$\cos(\frac{L}{\sqrt{2c}}\sqrt{1-\sqrt{1-4c\beta}}) = 0$$

In fact, the two cases lead to the same conclusion which gives

$$\frac{L}{\sqrt{2c}}\sqrt{1+\sqrt{1-4c\beta}} = (n+\frac{1}{2})\pi; \qquad (n=1,2,3...) \qquad (4.13)$$

From Eq. 4.11 we can obtain the eigenvalues β_n given by

$$\beta_n = \frac{(n+\frac{1}{2})^2\pi^2}{L^2}(1 - \frac{c}{L^2}(n+\frac{1}{2})^2\pi^2); \qquad (n=1,2,....) \qquad (4.14)$$

Because the restriction condition $0 < 4c\beta_n < 1$, the eigenvalues can only be a finite series instead of an infinite series. The number of terms of the series is determined from the relation .

$$N = \max\left[integer\left(\frac{L}{\sqrt{c}\pi} - \frac{1}{2}\right)\right] \qquad (4.15)$$

A finite series of proper orthogonal eigenfunctions exist in the high gradient theory, given by

$$X_n(x) = (\frac{2}{L})^{\frac{1}{2}}\sin[(n+\frac{1}{2})\frac{\pi}{L}x]; \qquad n = 0,1,2,...,N. \qquad (4.16)$$

From the above discussion, the waves smaller than certain wavelength can not exist in the high gradient medium due to the effect of internal length. The same conclusion was derived from the dispersion relation of granular media (Chang and Gao 1995b).

The maximum wave number and the minimum wavelength can be obtained from the restriction of non-negative eigenvalues. From Eq. 4.12, we obtain the maximum wave number

$$k_{max} = (N+\frac{1}{2})\frac{\pi}{L} \le \frac{1}{\sqrt{c}} \qquad (4.17)$$

or the minimum wavelength

$$\lambda_{min} = \frac{2\pi}{k_{max}} = 2\pi\sqrt{c} = C_0 r \qquad (4.18)$$

where $C_0 = 3.35\sqrt{\frac{5K_n + 2K_s}{3K_n + 2K_s}}$ is a constant.

For the limiting case of $K_s = 0$, the minimum wavelength is 3.45r, approximately two times of particle diameter, below which the waves can not propagate in the finite strip.

From the wave numbers obtained, we can deduce the natural frequencies given by

$$\omega_n = V\sqrt{\beta_n} = V\frac{(n+\frac{1}{2})\pi}{L}\sqrt{1 - \frac{c}{L}(n+\frac{1}{2})^2\pi^2}; \qquad n = 1,2,...,N. \qquad (4.19)$$

Corresponding to natural frequencies, the solution of Eq. 4.7a can be in the form

51

$$T_n = a_n \cos(\omega_n t) + b_n \sin(\omega_n t); \qquad n = 0,1,2,...,N. \tag{4.20}$$

Thus the solution of the wave propagation in the finite strip with a fixed end and free end is expressed as follows

$$u(x, t) = \sum_0^N (a_n \cos(\omega_n t) + b_n \sin(\omega_n t)) \sin[\frac{x}{L}(n+\frac{1}{2})\pi] \tag{4.21}$$

where coefficients a_n, b_n are to be determined from the initial conditions, given by

$$a_n = \frac{2}{L}\int_0^L u_0(x)\sin[\frac{x}{L}(n+\frac{1}{2})\pi]\, dx; \qquad n = 0,1,2,...,N.$$

$$b_n = \frac{2}{\omega_n L}\int_0^L v_0(x)\sin[\frac{x}{L}(n+\frac{1}{2})\pi]\, dx \tag{4.22}$$

4.4 WAVE PROPAGATION SUBJECT TO DYNAMIC TRACTION

In this section, we will consider wave propagation in the finite strip excited by the dynamic traction given by the boundary conditions Eqs. 4.4 and 4.5, with zero initial conditions. In this case, we propose the solution to be in the form

$$u(x,t) = Y(x,t) + \sum_0^N R_n(t)X_n(x) \tag{4.23}$$

where $X_n(x)$; $(n=0,1,...,N)$ are the eigenfunctions given by Eq. 4.16; and $Y(x,t), R_n(t)$; $(n=0,1,...,N)$ are the unknown functions.

Substituting Eq. 4.23 into the wave equation (4.3) leads to the following two differential equations:

$$\sum_0^N (\ddot{R}(t) + \omega_n^2 R(t))X_n(x) = -\frac{\partial^2 Y(x,t)}{\partial t^2}$$

$$c\frac{\partial^4 Y(x,t)}{\partial x^4} + \frac{\partial^2 Y(x,t)}{\partial x^2} = 0 \tag{4.24}$$

Next, multiplying both sides of Eq. 4.24a by $X_n(x)$, integrating over [0,L], and from the orthogonal property of eigenfunctions, we have

$$\ddot{R}_n(t) + \omega_n^2 R_n(t) = \ddot{\Phi}_n(t) \tag{4.25}$$

where

$$\Phi_n(t) = -\int_0^L Y(x, t)X_n(x)\, dx$$

For zero initial conditions, we obtain the solution of Eq. 4.25, given by

$$R_n(t) = \Phi_n(t) - \omega_n \int_0^L \Phi_n(\tau) \sin(\omega_n(t-\tau)) d\tau \qquad (4.26)$$

It is noted from Eq. 4.25b that we can approximately express the function

$$Y(x, t) = -\sum_0^N \Phi_n(t) X_n(x) \quad .$$

Substituting Eq.4.26 into Eq. 4.23 leads to the following form of the solution

$$u(x,t) = -\sum_{0^c} \omega_n X_n(x) \int_0^L \Phi_n(\tau) \sin(\omega_n(t-\tau)) d\tau \qquad (4.27)$$

In addition, the unknown function $Y(x, t)$ is determined from the static equation (4.24b). Its solution is

$$Y(x,t) = a(t) + b(t)x + c(t)\sin(\frac{x}{\sqrt{c}}) + d(t)\cos(\frac{x}{\sqrt{c}}) \qquad (4.28)$$

From the boundary conditions (4a),(5a) and (6b), we obtain that a=c=d=0. And then, from Eq. 4.4b, the solution of Eq. 4.24 becomes

$$Y(x,t) = \frac{xp(t)}{\lambda + 2\mu} \qquad (4.29)$$

Substituting Eq. 4.29 into Eq. 4.25b, we obtain

$$\Phi_n(t) = (-1)^{(n+1)} \frac{L\sqrt{2L}\, p(t)}{\pi^2(n+\frac{1}{2})^2} \qquad (4.30)$$

And then, substituting Eq. 4.30 into Eq. 4.27 leads to the final solution of wave propagation subject to dynamic traction, given by

$$u(x,t) = \frac{8L}{(\lambda + 2\mu)\pi^2} \sum_0^L \frac{(-1)^n \omega_n}{(2n+1)^2} \sin(\frac{x}{L}(n+\frac{1}{2})\pi) \int_0^t p(\tau)\sin(\omega_n(t-\tau)) d\tau \qquad (4.31)$$

For a specific time-dependent traction $p(t)$ given by

$$p(t) = P_0; \qquad 0 < t < t_0$$
$$= 0; \qquad t_0 < t \qquad (4.32)$$

53

The solution can be obtained by substituting Eq. 4.32 into Eq. 4.31, thus

$$u(x,t) = \frac{16 P_0 L}{(\lambda + 2\mu)\pi} \sum_0^L \frac{(-1)^n}{(2n+1)^2} \sin(\frac{x}{L}(n+\frac{1}{2})\pi) I(t) \qquad (4.33)$$

And then, the stress field is derived from the constitutive equation (4.2), given by

$$\sigma(x, t) = 8 P_0 \sum_0^N \frac{(-1)^n}{2n+1}(1 - \frac{c}{L^2}(n+\frac{1}{2})^2 \pi^2)\cos(\frac{x}{L}(n+\frac{1}{2})\pi) I(t) \qquad (4.34)$$

where

$$I(t) = \frac{1}{2}[1 - \cos(\omega_n t)]: \qquad 0 < t < t_0$$

$$= \sin(\omega_n \frac{t_0}{2})\sin(\omega_n(t - \frac{t_0}{2})); \qquad t_0 < t$$

4.5 SUMMARY

From Eq. 4.18, the admissible minimum wave length is proportional to the particle size. The number of terms of the harmonic waves propagating in granular materials is inversely proportional to the particle size. When the diameter of particles is very small compared to the , the effects of high gradient terms in the constitutive equation are negligible, and the solution of wave propagation is degenerated into classical solution.

In classical solution, all harmonic waves have the same wave velocity. In high gradient theory, each of harmonic wave has a different velocity. Since the excited wave due to dynamic traction is a summation of harmonic waves, the shape of the excited wave keeps constant during propagating in the classical theory. However, in high gradient theory, the shape of the excited wave changes due to dispersion.

Eq. 4.34 is used for analysing the stress wave propagating along the strip. A typical sequence of the stress wave propagation in the finite strip subjected to dynamic traction is shown in Fig. 4.1 using dimensionless variables.

Although the stress wave excited at the beginning of dynamic impact is only a simple compression wave, at later stage, the stress waves include both compression waves and extension waves. The phenomena is caused by the dispersion of stress waves due to the discrete nature of granular material.

The normalized peak of stress wave decay with time. The rate of decay decrease with time. The influence of particle size on the decay stress wave during propagation is shown in Fig. 4.2. When the particle diameter increase, the phenomenon of decay is a significant factor in the analysis of wave propagation in granular media.
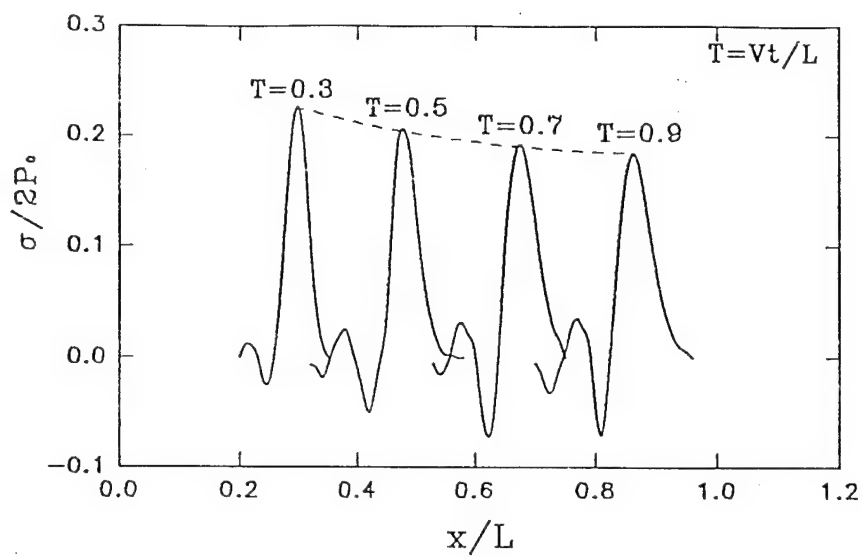
Figure 4.1   Stress wave propagates at different time
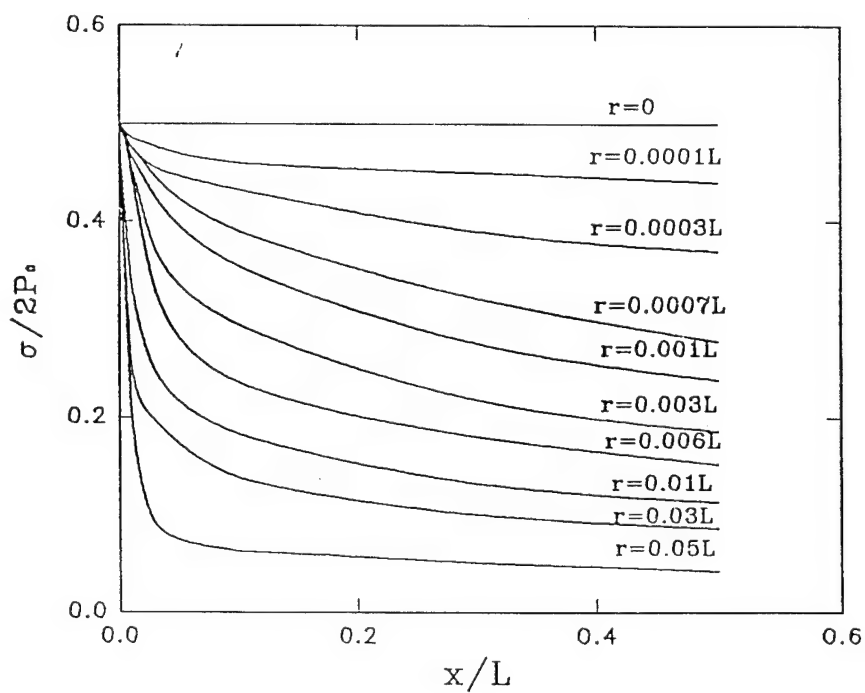
Figure 4.2   Influence of particle size on the decay of peak stress

CHAPTER 5
NORMAL AND TANGENTIAL COMPLIANCE FOR
ELASTIC CONFORMING BINDER CONTACT.

This chapter describes the normal and tangential conforming contact compliance for a system of two elastic particles bonded by a layer of elastic binder in between. The governing equation of this problem is a second kind of Fredlholm integral equation with singularities of logarithmic type. Exact solution for the unknown interfacial pressure between particle and binder is difficult to arrive. Derivations of compliance are presented in the forms of the upper and lower bounds, and of the best estimate based on physical approximations. It shows that the derived elastic compliances agree favorably with those of "discretized exact solutions" obtained from numerical methods.

5.1 INTRODUCTION

The subject of layer/binder contact frequently occurs in granular/particulate materials such as asphaltic concrete or cemented sand. This subject is also important in tribology, involving the mechanical behavior of coated materials. Many topics in this area have been investigated in the past years. For example, Muki (1960) studied the problem of contact between a layer and an elastic half space. Goodman and Keer (1975) studied a case of surface layers bounded to a substrate. Bentall and Johnson (1968) worked on a plane strain layered problem which was further studied by Meijers (1968) and Alblas and Kuipers (1970) for both conditions of thin and thick layers. Matthewson (1981) presented a theory of indentation of a soft thin coating by a rigid body. Keer et al. (1991) investigated the compliance of coated elastic bodies in contact. Dvorkin et al. (1991) employed numerical solutions to examine the normal interaction of two elastic spheres separated by an elastic cementation layer and recently (1994) extended the numerical solutions to examine tangential deformation of two cemented spheres. In addition, many related topics can be found in the books by Johnson (1985) and by Gladwell (1980).

This study is focused on the compliance of a system of two elastic particles bonded together by a thin layer of binder. We aim to derive closed-form relationships between the forces and the relative particle/binder movements in this system. Closed-form expressions are of particular interest because they can be readily incorporated into discrete element methods for the analysis of a large assembly of particles.

Progression of the chapter begins with establishing integral equations that govern the interfacial contact pressure distribution between particle and binder. Analyses of the upper and lower bounds with respect to the compliance of the two particle system are followed. The

56

best estimate of compliance based on physical approximation is then pursued. The closed-form analytical expressions are compared with the numerical solutions obtained directly from solving the governing integral equations by a discretization technique.

5.2 FORMULATION OF THE PROBLEM

Fig. 5.1 shows an axi-symmetric configuration of two particles bonded by a binder in a cylindrical coordinate. The function $z = h(r)$ represents the geometry of interfacial boundary between the particles and the binder, given by

$$h(r) = h_0\left(1 + d\frac{r^2}{a^2}\right) \tag{5.1}$$

where a is the radius of contact area, h_0 is the thickness of the binder at $r = 0$, and d is the dimensionless shape parameter related to the curvature of particle surface, which is limited in a range $0 \leq d < 1$. For a planer surface, d is zero. For a spherical particle, d is given by

$$d = \frac{a^2}{2Rh_0} \tag{5.2}$$

where R is the radius of the spherical particles.

We denote the constraint modulus E_1 and E_2, Poisson's ratio υ_1 and υ_2 for the particles and the binder respectively, where the constraint modulus E_1 and E_2 are defined as

$$E_i = \frac{2G_i(1 - \nu_i)}{1 - 2\nu_i}; \quad i = 1,2 \tag{5.3}$$

and G_1 and G_2 are the shear modulus of the particles and the binder respectively.

We intend to derive the normal and tangential compliance of this two particle system with an elastic binder. The governing equations that relate force and relative movement of two particles are discussed separately for the normal mode and the tangential mode.

5.2.1 Normal Compliance

The relative normal approach δ_z for the two contact bodies is separated into two components: the normal displacement at the binder-particle interface relative to the particle's centroid, $w_1(r)$; and the normal displacement at the binder-particle interface (i.e., at $z=h(r)$) relative to the $z=0$ plane, $w_2(r)$, given by

$$\delta_z = w_1(r) + w_2(r) \tag{5.4}$$

Since $z = 0$ is a plane of symmetry, the binder normal displacement vanishes at $z=0$. As the binder is a thin layer, we approximate the normal strain to be uniform in the z direction across the binder. Thus the normal displacement $w_2(r)$ contributed from binder can be expressed as

57

follows:

$$w_2(r) = h(r)\frac{p(r)}{E_2} \tag{5.5}$$

where p(r) is the interfacial normal pressure between the particles and the binder.

In the analysis of the normal displacement $w_1(r)$, we assume that the characteristic dimension of the particle is much larger than that of the particle-binder contact area. Thus it is justifiable to pursue the analysis of $w_1(r)$ based on a half-space premise. Following the well-known Boussinesq's equation, $w_1(r)$ can be related to p(r) by:

$$w_1(r) = \frac{(1 - v_1^2)}{\pi E_1} \int_0^a \int_0^{2\pi} \frac{p(\rho)\, \rho\, d\rho\, d\theta}{\sqrt{r^2 + \rho^2 - 2r\,\rho\,\cos\theta}} \tag{5.6}$$

Substituting Eqs. 5.5 and 5.6 into Eq. 5.4, we have

$$\delta_z = h(r)\frac{p(r)}{E_2} + \frac{(1 - v_1^2)}{\pi E_1} \int_0^a \frac{p(\rho)\, \rho\, I(\rho,r)\, d\rho}{\sqrt{r^2 + \rho^2}} \tag{5.7}$$

where I(ρ, r) are defined as

$$I(\rho,r) = I(k) = \int_0^{2\pi} \frac{d\theta}{\sqrt{1 - k\cos\theta}} \quad ; \quad k = \frac{2r\rho}{r^2 + \rho^2} \tag{5.8}$$

Integration of the interfacial pressure function, p(r), over the contact area gives the resultant normal contact force P_z

$$P_z = 2\pi \int_0^a p(r)r\, dr \tag{5.9}$$

Eqs. 5.7 and 5.9 indirectly provide the compliance relationship between the relative normal approach δ_z and the contact force P_z through the interfacial pressure function.

5.2.2 Tangential Compliance

The relative tangential approach in the x-direction δ_x for the two contact bodies is also separated into two components: the tangential displacement at the binder-particle interface relative to the particle's centroid, $u_1(r, \theta)$; and the tangential displacement at the binder-particle interface (i.e., at z = h(r)) relative to the z = 0 plane, $u_2(r, \theta)$, given by

$$\delta_x = u_1(r,\theta) + u_2(r,\theta) \tag{5.10}$$

The tangential displacement vanishes at the plane of symmetry z = 0. Considering that the binder is a thin layer, we approximate the tangential strain to be uniform in the z direction across the binder, and the following relation can then be derived:

$$u_2(r,\theta) = h(r)\frac{q(r,\theta)}{G_2} \tag{5.11}$$

where G_2 is the shear modulus of binder, q(r, θ) is the interfacial tangential pressure between

the particles and the binder.

Since the characteristic dimension for the particle is much larger than that of the contact area, we use the known relationship between $u_1(r, \theta)$ and $q(r, \theta)$ based on the half-space premise (Johnson 1985). Thus the tangential displacement δ_x for the two contact bodies is now equal to the summation of $u_1(r, \theta)$ and $u_2(r, \theta)$ with an error of the order $(\upsilon_1)^2$ (Dvorkin et al., 1994)

$$\delta_x = h(r)\frac{q(r, \theta)}{G_2} + \frac{1}{2\pi G_1} \int_0^a \int_0^{2\pi} q(\rho,\phi)\ F(r,\rho,\theta,\phi,\nu_1)\rho\,d\phi\,d\rho \qquad (5.12)$$

where

$$F(r,\rho,\theta,\phi,\nu_1) = \{\frac{1-\nu_1}{\xi} + \nu_1\ \frac{(r\cos\theta-\rho\cos\phi)^2}{\xi^3}\} \qquad (5.13)$$

$$\xi^2 = (r\cos\theta - \rho\cos\phi)^2 + (r\sin\theta - \rho\sin\phi)^2$$

where, G_1 and υ_1 are respectively the shear modulus and Poisson's ratio of the particle. Integration of the interfacial pressure function, $q(r, \theta)$, over the contact area gives the resultant tangential contact force P_x

$$P_x = \int_0^a \int_0^{2\pi} q(r,\theta)r\ d\theta\ dr \qquad (5.14)$$

Again the governing equations (12) and (14) provide the compliance relationship between the relative tangential approach δ_x and the contact force P_x through the unknown interfacial pressure function, $q(r, \theta)$.

In fact, the interfacial pressure functions, $q(r, \theta)$ or $p(r)$, can be determined by simultaneously solving Eqs. 5.12 and 5.14 or Eqs. 5.7 and 5.9. Unfortunately, the governing equations (7) and (12) are the second kind of Fredholm integral equations with kernels which have logarithmic singularities. To this type of integral equations, analytical solutions are difficult to arrive. However, with special care on the singularities, they can be solved using a numerical discretization technique. Details can be found in Zhu et al (1995).

5.3 SOLUTIONS FOR TWO EXTREME CASES

The analytical solutions of the interfacial pressures $p(r)$ in Eq. 5.7 and $q(r, \theta)$ in Eq. 5.12 are known for two extreme cases, namely, (1) rigid particle case (i.e., $E_1 \rightarrow \infty$ and $G_1 \rightarrow \infty$ while E_2 and G_2 are finite), and (2) rigid binder case (i.e., E_1 and G_2 are finite while $E_2 \rightarrow \infty$ and $G_1 \rightarrow \infty$). The compliance relationship under these two extreme conditions are described in this section.

59

Rigid Particle Case

In the rigid particle case, the relative movement of the two contact bodies is contributed only from the deformation of binder. Thus

$$\delta_z = h(r) \frac{p(r)}{E_2} \tag{5.15}$$

$$\delta_x = h(r) \frac{q(r,\theta)}{G_2} \tag{5.16}$$

Subsequently, for the rigid particle case, the corresponding normal interfacial pressure denoted as $p_1(r)$ is given by

$$p_1(r) = \frac{P_z}{\pi a^2} \frac{h_0}{h(r) X} \tag{5.17}$$

and the interfacial tangential pressure $q(r, \theta)$ becomes independent of the variable θ (denoted as $q_1(r)$) and reads

$$q_1(r) = \frac{P_x h_0}{\pi a^2 h(r) X} \tag{5.18}$$

where

$$X = \frac{\ln(1+d)}{d} \tag{5.19}$$

and d is the shape parameter defined in Eq. 5.1.

Thus the normal and tangential compliance relationships between the contact force P_z and the relative approach δ_z become

$$\delta_z = C_{1z} P_z \quad ; \quad C_{1z} = \frac{h_0}{\pi a^2 E_2 X} \tag{5.20}$$

$$\delta_x = C_{1x} P_x \quad ; \quad C_{1x} = \frac{h_0}{\pi a^2 G_2 X} \tag{5.21}$$

Rigid Binder Case

In the rigid binder case, which represents the well known rigid punch problem, the normal interfacial pressure, denoted as $p_2(r)$, is given by

$$P_2(r) = \frac{P_z}{2\pi a^3} (a^2 - r^2)^{-\frac{1}{2}} \tag{5.22}$$

and the tangential pressure, $q(r, \theta)$ is again dependent only on r (denoted as $q_2(r)$):

$$q_2(r) = \frac{P_x}{2\pi a} (a^2 - r^2)^{-\frac{1}{2}} \tag{5.23}$$

For this case, the normal and tangential compliances are:

$$\delta_z = C_{2z}P_z \quad ; \quad C_{2z} = \frac{1-v_1^2}{2aE_1} \tag{5.24}$$

$$\delta_x = C_{2x}P_x \quad ; \quad C_{2x} = \frac{2-v_1}{8aG_1} \tag{5.25}$$

It can be easily verified that under both extreme conditions, $r\, p_1(r)$, $r\, p_2(r)$, $r\, q_1(r)$, and $rq_2(r)$, are monotonically decreasing functions in the range of $0 < r < a$. Indeed, the functions $r\, p(r)$ and $r\, q(r)$ are monotonic for any pairs of E_1, E_2 and G_1, G_2 as verified from the numerical method given in Appendix-A.

5.4 UPPER BOUND SOLUTION

Explicit compliance relationships are easily derived for the two extreme conditions. However, for general conditions, analytical solutions to Eq. 5.7 and Eq. 5.12 are difficult to obtain. The upper and lower bounds, and the best estimated solution based on the physical approximations have been derived by Zhu et. al (1995). A brief summary is given in this section.

The governing equations are first transformed to be suitable for the use of *Chebyshev's inequality for integral.* Using the principles of *Chebyshev's inequality for integral,* the equations can be greatly simplified thus leading to the upper bound solution for the normal compliance

$$\delta_z \leq (C_{1z} + b_1 C_{2z}) P_z \tag{5.26}$$

where

$$b_1 = \frac{2H(d)}{\pi^2 X} \tag{5.27}$$

$$H(d) = 5.699 - 2.404d + 1.495d^2 - 1.079d^3 + 0.841\, d^4 - 0.689 \frac{d^5}{1+d} \tag{5.28}$$

and the upper bound solution for the tangential compliance:

$$\delta_x \leq (C_{1x} + C_{2x} \frac{2b_1}{2-v_1}) P_x \tag{5.29}$$

where, b_1 is defined in Eq. 5.27.

5.5 LOWER BOUND SOLUTION

Similarly, application of the *Chebyshev's inequality for integral* results in the lower bound solution for the normal compliance:

$$\delta_z \geq (b_2 C_{1z} + C_{2z}) P_z \qquad (5.30)$$

where

$$b_2 = \frac{\pi}{4}(1 + 0.5d)X < 1 \qquad (5.31)$$

and the lower bound solution for the tangential compliance:

$$\delta_x \geq (b_2 C_{1x} + C_{2x}) P_x \qquad (5.32)$$

Based on the upper and lower bound solutions, the true normal compliance must be between $(C_{1z} + b_1 C_{2z})$ and $(b_2 C_{1z} + C_{2z})$, and the true tangential compliance must be between $(C_{1x} + b_1 C_{2x})$ and $(b_2 C_{1x} + C_{2x})$. Examining the range of values of b_1 and b_2, for versus the shape parameters, the maximum relative difference between the upper and lower bounds of compliance is from 18-20 %.

5.6 BEST ESTIMATE BASED ON PHYSICAL APPROXIMATIONS

Based on physical approximation, it leads to the following best estimate for normal and tangential compliance relationship:

$$\delta_z = (C_{1z} + C_{2z}) P_z \qquad (5.33)$$

$$\delta_x = (C_{1x} + C_{2x}) P_x \qquad (5.34)$$

Eqs. 5.33 and 5.34 satisfy the two extreme cases: (1), rigid particle case ($E_1 \rightarrow \infty$ and E_2 finite); and (2), rigid binder case (E_1 finite and $E_2 \rightarrow \infty$). In addition, the best estimated compliances fall in between the upper and lower bounds, i.e., the following inequalities are always satisfied:

$$b_2 C_1 + C_2 < C_1 + C_2 < C_1 + b_1 C_2 \qquad (5.35)$$

$$b_2 C_{1x} + C_{2x} < C_{1x} + C_{2x} < C_{1x} + \frac{2b_1}{2 - v_1} C_{2x} \qquad (5.36)$$

Eqs. 5.33 and 5.34 indicate that the overall compliance corresponds to a serial connection of the two compliances C_1 and C_2, where C_1 represents the compliance of particle and C_2 represents the compliance of binder. The best estimated analytical compliances are in good agreement with the compliances numerically calculated (Zhu et al 1995).

5.7 SUMMARY

For the compliance of an elastic particle-binder system, the governing equation is a second kind of Fredholm integral equation with singularities of logarithmic type. Exact solution is difficult to arrive. Even solved numerically, special care needs to be taken for the convergency problems associated with the singularities. This approach makes a use of the principles of *Chebyshev's inequality for integral* which allows simplifications of the governing equations thus yields remarkably simple closed-form expressions for the upper and lower bound solutions of compliances. The best estimates of compliances have been found to be favorably in agreement with the numerical solutions and thus can be considered as a good approximate solution for this type of problem.
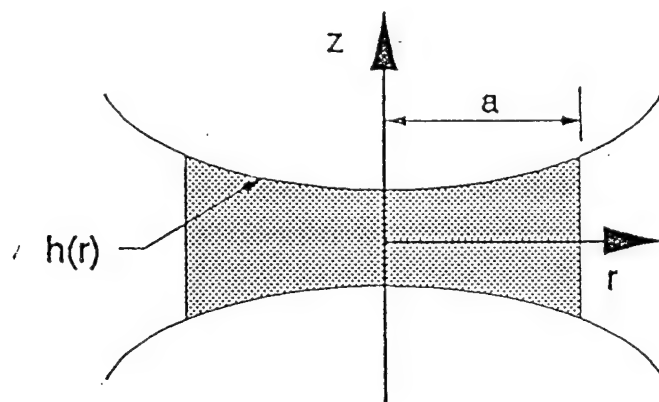
Figure 5.1 Sketch of the configuration for a binder-particle system

CHAPTER 6
SUMMARY AND CONCLUSION

This report reviews the results of this project in four different areas: 1) descriptions of micro-structure, 2) micro-macro relationship, 3) classes of micromechanics constitutive theory, and 4) contact law of the inter-particle binder. These four areas are essential to the construction of a micromechanics theory for particulate media.

Chapter two describes several methods of micro-structure characterization and how the microstructure description is integrated in the formulation to relate the micro-macro mechanical behavior. The discrete variables selected in the micromechanics model depend greatly on the type of micro-structure descriptor. Thus the micro-structure descriptor is the key element in micromechanics theory for granular material. The cell model, as oppose to the branch model, is found to be useful in describing spacial variation of microstructure (i.e., the heterogeneity of material). However, there are still many fundamental issues need to be resolved on the mechanics of cell interaction.

Chapter three addresses the limitation of classic continuum in modelling granular media. In order to model some features due to the effect of microstructure and discrete nature of granular particles, generalized continua different from the classic continuum are necessary to be considered. Several new classes of generalized continua, ranging from simple to complex, are derived for representing granular media. Degree of complexity of the continuum is proportional to the modelling capability. For example the micro-polar continua is useful in modelling the effect of particle rotation. The high gradient model is useful in modelling large deformation especially after peak strength of the granular material and in modelling some distinct features for dynamic wave propagating through granular media.

In Chapter four, the high gradient model is used as an example to analyze the wave dispersion in granular media, a phenomenon that can not be modelled by the classic continua. The results show that waves with different frequencies have different velocities in a granular medium. Short waves propagate slower. Very short waves can not pass through the medium. Subsequently, a relationship is derived for the decay of peak stress wave as a function of particle size. This phenomenon is very different from the theory of wave propagating in classic continuum.

Chapter five presents part of the results from the collaborated work with Wright laboratory at Tyndall Air Force Base. This chapter describes the normal and tangential conforming contact compliance for a system of two elastic particles bonded by a layer of elastic binder in between. The principle of Chebyshev's inequality is found to be a useful concept for obtaining solutions for the governing equations of Fredlholm type. Continuation of the work are undertaken for studying compliance of a binder/particle system in rolling and twisting modes.

REFERENCES

Alblas, J.B. & Kuipers, M. (1970), "On the Two-dimensional Problem of a Cylindrical Stamp Pressed into a Thin Elastic Layer", *Acta Mechanica*, Vol. 9, 292.

Bathurst, R. J. and Rothenberg, L. (1988), "Micromechanical Aspects of Isotropic Granular Assemblies with Linear Contact Interactions", *Journal of Applied Mechanics,* ASME, Vol. 55, 17-23.

Bardenhagen, S. and Trianfyllidis, N. (1994)," Derivation of Higher Order Gradient Continuum Theories in 2,3-D Non-linear Elasticity from Periodic Lattice Models", *Journal of Mechanics and Physics of Solids*, Vol. 42, 111-139.

Bazant, Z. P. and Pijaudier-Cabot, G (1987), "Nonlocal Continuum Damage Localization Instability and Convergence" *Journal of Applied Mechanics*, ASME, Vol. 55, 659-673.

Beesack, P.R. and Pecaric, J.E. (1985). "Integral Inequalities of Chebyshev Type," *J. Math. Analysis Applications*, Vol. 111, 643-659.

Bentall, R.H. & Johnson, K.L. (1968), "An Elastic Strip in Plane Rolling Contact," *Int. J. of Mechanical Sciences*, Vol. 10, 637.

Beran, M. J. and McCoy, J. J. (1970a), "Mean Field Variations in a Statistical Sample of Heterogeneous Linearly Elastic Solids", *International Journal of Solids and Structures* Vol. 6, 1035-1054.

Beran, M.J. and McCoy, J.J. (1970b), "The Use of Strain Gradient Theory for Analysis of Random Media" *International Journal of Solids and Structures*, Vol. 6,1267-1275

Cambou, B. (1993), "From Global to Local Variables in Granular Material," *Powders and Grains*, C. Thornton, ed., A. A. Balkema, Rotterdam, The Netherlands, 73-86.

Chang, C.S. (1988), "Micromechanical Modelling of Constitutive Relations for Granular Material", Micromechanics of Granular Materials, Eds. M. Stake, and J.T.Jenkins, Elsevier, Amsterdam, The Netherlands, 271-279.

Chang, C. S. (1993), "Micromechanics Modeling for Deformation and Failure of Granulates with Frictional Contacts," *Mechanics of Material*, Elsevier Science Publishers, Amsterdam, Vol. 16, No.1-2, pp. 13-24.

Chang, C. S., Misra, A., and Acheampong, K. (1992), "Elastoplastic Deformation of Granulates with Frictional Contacts," *Journal of Engineering Mechanics*, ASCE, Vol. 118, No. 8, pp. 1692-1708.

Chang, C. S., and Gao, J. (1995a), "Second-Gradient Constitutive Theory for Granular Material with Random Packing Structure," *International Journal of Solids and Structures*, Vol. 32 (in print).

Chang, C. S. and Gao, J. (1995b), "Non-linear Dispersion of Plane Wave in Granular Media," *Journal of Non-linear Mechanics*, (in print).

Chang, C.S. and Liao, C. (1990), "Constitutive Relations for Particulate Medium with the Effect of Particle Rotation", *International Journal of Solids and Structures*, Vol. 26, 437-453.

Chang, C. S and Ma, L. (1991), "A Micromechanical-based Micro-polar Theory for Deformation of Granular Solids", *International Journal of Solids and Structures*, Vol. 28, 67-86.

Chang, C.S. and Ma, L. (1992), "Elastic Material Constants for Isotropic Granular Solids with Particle Rotation", *International Journal of Solids and Structures*, Vol.29, 1001-1018.

Chang, C. S. and Misra, A. (1989), "Theoretical and Experimental Study of Regular Packings of Granules," *Journal of Engineering Mechanics*, ASCE, Vol. 115, No. 4, pp. 704-720.

Christoffersen, J., Mehrabadi, M.M. and Nemat-Nassar, S. (1981), "A Micromechanical Description on Granular Material Behavior", *Journal of Applied Mechanics*, ASME, Vol.48, 339-344.

Coleman, B.D. and Hodgdon, M.L. (1985), "On Shear Bands in Ductile Materials" Arch. Ret. Mech. Anal. Vol. 90, 219-247.

Cosserat, E and F. (1909), "Theorie des Corps Deformables" A Herman et Fils, Paris.

Deresiewicz, H. (1958), "Stress-Strain Relations for A Simple Model of a Granular Medium", *Journal of Applied Mechanics,* Vol.25, 402-406.

Dvorkin, J., Mavko, G. and Nur, A. (1991), "The Effect of Cementation on the Elastic Properties of Granular Material," *Mechanics of Materials*, Vol. 12, 207-217.

Dvorkin, J., and Yin, Hezhu (1994), "Contact Laws for Cemented Grains: Implications for Grain and Cement Failure", *Mechanics of Materials*, to be appeared.

Duffy, J. (1959), "A Differential Stress-Strain Relation for the Hexagonal Close Packed Array", *Journal of Applied Mechanics*, ASME, Vol. 26, 88-94.

Duffy, J. and Mindlin, R. D. (1957), "Stress-Strain Relation and Virbrations of a Granular Media", *Journal of Applied Mechanics*, ASME, Vol. 24, 593-595.

Eringen, A. E. (1968). Theory of Micropolar Elasticity. In Fracture - An Advanced Treatise (Edited by H. Liebowitz), Vol. II, Chapter 7, pp. 621-693. Academic Press, New York.

Eringen, A. C. and Edelen, D. G. B. (1972), "On Nonlocal Elasticity" *International Journal Engineering Science*, Vol.10, 233-248.

Eringen, A.C. (1973), "Linear Theory of Nonlocal Microelasticity and Dispersion of Plane Waves" Letter of Applied Science, Vol.1, 129-146.

Gladwell, G.M.L. (1980). Contact Problems in the Classical Theory of Elasticity Alphen aan den Rijn: Sijthoff and Noordhoff.

Goodman, L.E. and Keer, L.M. (1975), "Influence of an Elastic Layer on the Tangential Compliance of Bodies in Contact", *The Mechanics of the Contact Between Deformable Bodies* (Edited by A.D. de Pater and J.J. Kalker), 127-151, Delft University Press.

Jenkins, J. T. (1988), "Volume Change in Small Strain Axisymmetric Deformations of a Granular Material", *Micromechanics of Granular Materials*, Eds. M. Satake, and J.T. Jenkins, Elsevier, Amsterdam, The Netherlands, 143-152.

67

Jenkins, J. T. and Strack, O. D. L. (1993), "Mean Field Stress-strain Relations for Random Arrays of Identical Spheres in Triaxial Compression," Advances in Micromechanics of Granular Materials, Eds., Shen et. al., Elsevier, Amsterdam, 41-50.

Johnson, K.L. (1985). *Contact Mechanics*, Cambridge University Press, Cambridge.

Keer, L.M., Kim, S.H., Eberhardt, A.W., and Vithoontien, V. (1991). Compliance of Coated Elastic Bodies in Contact. *Int.J. Solids Structures*, Vol. 27, No. 6, 681-698.

Kroener, E. (1967), "Elasticity Theory of Materials with Long Range Cohesive Forces" *International Journal of Solids and Structures*. Vol.3, 731-742.

Koenders, M. A. (1987), "The Incremental Stiffness of an Assembly of Particles," *Acta Mechanica*, Vol. 70, 31-49.

Lee, J.S., Ma, M.Y., and Huang, A.B. (1992), "Micromechanical Simulation of Wave Propagation in Dense Granular Assemblies", *Engineering Mechanics* (Proceedings of Ninth Conference ASCE) Eds. L. D. Lutes and J.M. Niedzwecki, ASCE. New York, 417-420.

Koenders, M. A. (1994), "Least Square Methods for the Mechanics of Nonhomogeneous Granular Assemblies," *Acta Mechanica*, Springer- Verlag, Vol. 107.

Levin, V. M. (1971), "The Relation Between Mathematical Expectations of Stress and Strain Tensors in Elastic Microheterogeneous Media," PMM, Vol. 35, No. 4, 744-750.

Mattewson, M.J. (1981), "Axi-symmetric Contact on Thin Compliant Coatings", *J. Mech. Phys. Solids,* Vol. 29, 89.

Meijers, P. (1968), "The Contact Problem of a Rigid Cylinder on an Elastic Layer", *Applied Science Research*, Vol. 18, 353.

Mindlin, R. D. and Tiersten, H. F. (1962), "Effects of Couple Stresses in Linear Elasticity", *Arch.Rat. Mech. Anal.* Vol.11, 415-421.

Mindlin, R. D. (1965), "Second Gradient of Strain and Surface-Tension in Linear Elasticity", *International Journal of Solids and Structures*, Vol.1. 417-438.

Muki, R. (1960), "Asymmetric Problems of the Theory of Elasticity for a Semi-infinite Solid and a Thick Plate", *Progress in Solid Mechanics* (Edited by I. N. Sneddon and R. Hill), Vol. 1, North-Holland, Amsterdam.

Rothenberg L. and Selvadurai, A. P. S. (1981), "Micromechanical Definition of the Cauchy Stress Tensor for Particulate Media", *Mechanics of Structured Media* (ed. A.P.S. Selvadurai), Elsevier, Amsterdam, The Netherlands, pp. 469-486.

Sadd, M. H., Tai, Q. and Shukla, A.(1992), " Contact Law Effects on Wave Propagation inParticula te Materials Using Distinct Element Modelling", *International Journal of Nonlinear Mechanics.*, Vol. 28, 251-265

Shukla, A., and Sadd, M.H., and Mei, H.(1991), "Experimental and Computational Modelling of Wave Propagation in Granular Materials", *Exp. Mech.* Vol. 30, 377-381

Thornton, C. and Randall, C.W.,(1988), "Applications of Theoretical Contact   Mechanics to Solid Particle System Simulation", *Micromechanics of Granular Materials*, Eds. M. Stake, and Jenkins, J.T. Elsevier, Amsterdam, The Netherlands, 133-142.

Toupin, R. A. (1962), "Elastic Materials with Couple-Stresses", *Arch. Rat. Mech.Anal.*, Vol.11 385-396

Toupin, R. A. and Gazis, D. C. (1964), "Surface Effects and Initial Stress in Continuum and Lattice Models of Elastic Crystals" in *Proceedings of the International Conference on Lattice Dynamics*, Ed by Walli, R. F, Pergamon Press, 594-602

Triantafyllidis, N. and Aifantis, E. C. (1986), "A Gradient Approach to Localization of Deformation I-Hyperelastic Materials", *Journal of Elasticity*, Vol.16, 225-237

Truesdell, C. and Toupin, R.A. (1960), "The Classical Field Theories", *Encyclopedi of Physics*, Vol III/1 Springer-Verlag, Berlin

Walton, K. (1987), "The Effective Elastic Moduli of a Random Packing of Spheres", *Journal of Mechanics and Physics of Solids*, Vol.35, 213-226.

Weyl, H. (1944). Classical Groups. Princeton University Press.